Expansion of coccidioidomycosis endemic regions in the United States in response to climate change

Morgan E. Gorris[1], Kathleen K. Treseder[2], Charles S. Zender[1], and James T. Randerson[1]

[1]Department of Earth System Science, University of California, Irvine, California, USA
[2]Department of Ecology and Evolutionary Biology, University of California, Irvine, California, USA

Corresponding author: Morgan E. Gorris (mgorris@uci.edu)

Key Points:

- We created a niche model to estimate climate limits on the spatial extent of Valley fever endemicity in the United States
- For a high warming scenario, the area of climate-limited endemicity will more than double by 2100, expanding northward into dry western states
- Our predictive model of Valley fever endemic regions may help mitigate disease impacts as the disease spreads into new regions

Abstract

Coccidioidomycosis (Valley fever) is a fungal disease endemic to the southwestern United States. Across this region, temperature and precipitation influence the extent of the endemic region and number of Valley fever cases. Climate projections for the western US indicate temperatures will increase and precipitation patterns will shift, which may alter disease dynamics. We estimated the area potentially endemic to Valley fever using a climate niche model derived from contemporary climate and disease incidence data. We then used our model with projections of climate from Earth system models to assess how endemic areas will change during the 21st century. By 2100 in a high warming scenario, our model predicts the area of climate-limited endemicity will more than double, the number of affected states will increase from 12 to 17, and the number of Valley fever cases will increase by 50%. The Valley fever endemic region will expand north into dry western states, including Idaho, Wyoming, Montana, Nebraska, South Dakota, and North Dakota. Precipitation will limit the disease from spreading into states farther east and along the central and northern Pacific coast. This is the first quantitative estimate of how climate change may influence Valley fever in the US. Our predictive model of Valley fever endemicity may provide guidance to public health officials to establish disease surveillance programs and design mitigation efforts to limit the impacts of this disease.

Plain Language Summary

Valley fever is a fungal disease most common in the southwestern United States. Generally, the disease is limited to areas that are hot and dry. Climate change will cause the western US to become hotter and may change the location, timing, and amount of rain. This is

38 likely to change which counties are affected by Valley fever. We used climate observations to
39 estimate which counties in the US have a higher risk for Valley fever. Then, we used predictions
40 of future climate to map which counties may become affected by Valley fever during the
41 remainder of the 21st century. By 2100, our model predicts the area affected by Valley fever will
42 more than double and the number of people who become sick will increase by 50%. The area
43 affected by Valley fever will expand north into drier states in the western US, including Idaho,
44 Wyoming, Montana, Nebraska, South Dakota, and North Dakota. Our estimate may help public
45 health officials develop more effective plans so less people suffer from this disease.
46

47 **Introduction**

48 Coccidioidomycosis, commonly known as Valley fever, is an infectious fungal disease
49 that has gained attention in the United States due to a recent increase in cases (CDC, 2018a).
50 Humans contract Valley fever when they inhale *Coccidioides* spp. fungal spores. At onset,
51 symptoms of Valley fever closely resemble the flu, which may delay diagnosis (CDC, 2018b). If
52 left untreated, debilitating symptoms may occur, and on rare occasion may cause death. Valley
53 fever is not a communicable disease, so cases are a result of human exposure to *Coccidioides*
54 spp. in the environment.

55 *Coccidioides* spp., and therefore Valley fever, is endemic to the southwestern United
56 States and parts of Central and South America (CDC, 2017). Currently, there are two known
57 species of *Coccidioides*, both of which cause Valley fever: *C. immitis* and *C. posadasii* (Lauer,
58 2017). *C. immitis* is thought to be the primary species present in California, while *C. posadasii*
59 has a broader geographic distribution and is more commonly found in the highly endemic areas
60 of Arizona (Barker et al., 2019; Lauer, 2017). The fungi grow as hyphae within desert soils

(Stewart & Meyer, 1932). As such, *Coccidioides* spp. growth and abundance are influenced by environmental conditions (Maddy, 1957). The fungi proliferate during wet periods. When water becomes limiting, *Coccidioides* spp. hyphae then break apart into spore-containing fragments, small enough for humans to inhale (Maddy, 1957). Any type of soil disturbance, like high winds or digging in dry soils, can cause *Coccidioides* spp. spores to become airborne and potentially inhaled by humans. Many details about the *Coccidioides* spp. life cycle and the microecosystem characteristics that structure its presence in soils are unknown. As a consequence, environmental surveillance for the fungi has yielded relatively few soil samples that have tested positive for *Coccidioides* spp.

Because the fungi have not been systematically mapped across the hypothesized endemic region, much of our understanding of the relationships between environmental factors and *Coccidioides* spp. comes from studying epidemiological data. On a regional scale, weather and climate are known to influence the seasonal and interannual variability of disease incidence. Previous studies support a pattern of wet, then dry conditions preceding increased Valley fever incidence across the southwestern US (Comrie, 2005; Coopersmith et al., 2017; Gorris et al., 2018; Kolivras & Comrie, 2003; Komatsu et al., 2003; Park et al., 2005; Talamantes et al., 2007; Tamerius & Comrie, 2011; Zender & Talamantes, 2006). These dual controls first increase fungal growth during periods of higher than normal moisture. Then, they increase spore production and effective dispersal when hot temperatures and low rainfall desiccate soils and enhance the production of dust. Time delays between drying and elevated levels of incidence are observed in the two highly endemic regions, the San Joaquin Valley of California and south-central Arizona, despite regional differences in the timing of precipitation (Gorris et al., 2018). On finer temporal and spatial scales, processes such as soil disturbance, dust storms, and

84 agricultural activity can also influence Valley fever incidence (Tong et al., 2017; Williams et al.,
85 1979; Wilken et al., 2015).

86 These connections between climatic conditions and disease dynamics suggest on regional
87 scales, climate may also structure the environmental range of the fungi, and therefore the spatial
88 extent of Valley fever endemicity (Baptista-Rosas et al., 2007; Fisher et al., 2007). Two main
89 climate conditions that regulate the occurrence of *Coccidioides* spp. in the environment are
90 temperature and precipitation (Baptista-Rosas et al., 2007; Fisher et al., 2007; Gorris et al.,
91 2018). County-level Valley fever case reports from 2000-2015 across 5 states in the
92 southwestern US revealed the spatial pattern of incidence has a non-linear positive relationship
93 with mean annual temperature and non-linear inverse relationship with mean annual precipitation
94 (Gorris et al., 2018). Ultimately, these two climate conditions structure the presence of deserts:
95 the biome in which *Coccidioides* spp. thrives (Fisher et al., 2007; Maddy, 1957). High
96 temperatures may limit the growth of many microbial competitors, allowing *Coccidioides* spp. to
97 more effectively compete for soil resources (Barker et al., 2012; Greene et al., 2000). Low levels
98 of precipitation in deserts may also limit microbial competitors; however, occasional periods of
99 high moisture availability are important for *Coccidioides* spp. fungal growth and reproduction
100 (Fisher et al., 2007; Maddy, 1957). In contrast, wet soils in regions with high mean annual
101 precipitation may limit dust production, spore dispersal, and thus human exposure to
102 *Coccidioides* spp. (Gorris et al., 2018).

103 There is also preliminary evidence from the few soil samples positive for *Coccidioides*
104 ssp. that temperature and precipitation may be important for structuring the spatial pattern of
105 Valley fever endemicity. Most soil samples positive for *Coccidioides* ssp. were collected from
106 the Central Valley of California (Colson et al., 2017; Lauer et al., 2012; 2014), south-central

Arizona (Barker et al., 2012), and Baja Mexico (Baptista-Rosas et al., 2012; Catalán-Dibene et al., 2014; Vargas-Gastelum et al., 2015)—all areas that are hot and dry. Nineteen soil samples positive for *Coccidioides* ssp. and measures of both temperature and precipitation along with a large suite of other bioclimatic variables were used in the first known statistical environmental niche model of *Coccidioides* ssp. in northwestern Mexico and parts of the southwestern US (Baptista-Rosas et al., 2007). This model identified the most likely habitat for *Coccidioides* spp. as the Lower Sonoran Desert habitat and successfully highlighted epidemiological hotspots of Valley fever in the Central Valley of California and south-central Arizona. However, the niche model derived from this set of observations cannot fully explain the current spatial pattern of Valley fever cases (CDC, 2018b). This may be a consequence of the relatively small number of soil samples used to initialize the model. Until soils are systematically sampled across the western US, epidemiological data may provide a more robust way of delineating the effects of temperature and precipitation on the regions endemic for Valley fever.

Climate change is increasing temperatures and shifting precipitation patterns throughout the US. These changes could alter the regions endemic to Valley fever, as well as the number of Valley fever cases. Temperatures in the contiguous US are expected to increase by 1.6–6.6°C by 2100 (relative to 1986–2015) under a high greenhouse gas emissions scenario, representative concentration pathway 8.5 (RCP8.5; Hayhoe et al., 2018). This warming may allow *Coccidioides* spp. to expand its geographical range farther north, in areas previously unsuitable for the species to survive. Precipitation projections are more uncertain for the western US, and changes will likely vary by region and season (Easterling et al., 2017; Hayhoe et al., 2018; Swain et al., 2018). Along the Pacific coast, especially in the Pacific Northwest, mean annual precipitation is projected to increase (Easterling et al., 2017; Hayhoe et al., 2018). In contrast, the southwestern

US will likely experience little to no change in precipitation, while the southern Great Plains may become drier. In dry areas, increasing temperatures will likely increase evaporative demand, which may contribute to desertification. The expansion of dryland ecosystems may increase the area suitable for the occurrence of *Coccidioides* spp., along with the production of dust and fungal spores.

To predict how climate change may influence the spatial pattern of Valley fever in the future, it is important to have an accurate map of the current endemic area. The basis of the US Centers for Disease Control and Prevention (CDC) estimate of endemic areas is a historical skin test study of approximately 88,000 young men at a Naval Training Center in San Diego, CA from 1948–1950 that detected exposure to *Coccidioides* spp. (CDC, 2018b; Edwards & Palmer, 1957). Since the original study, the endemicity map has been modified to account for localized outbreaks of Valley fever (Marsden-Huag et al., 2012; Peterson et al., 2004; Werner & Pappagianis, 1973; Werner et al., 1972). One outbreak caused by *C. immitis* occurred in Washington State, well outside its normal geographical range in the Central Valley of California, and outside the hypothesized endemic region of Valley fever throughout the southwestern US (Litvintseva et al., 2014; Marsden-Huag et al., 2012).

More recently, a county-level map of mean annual Valley fever incidence derived from sixteen years of epidemiological data collected from state health agencies provided an independent way to estimate endemic areas (Gorris et al., 2018). This incidence database has not been used with niche modeling to explore the spatial pattern of disease. Valley fever case reports alone may be an underestimate of the actual burden of disease due to misdiagnosis, underreporting, or other host factors (Ampel, 2010; Chang et al., 2008; Jones et al., 2017). Despite this limitation, further analysis of epidemiological data may provide a means to better

153 estimate where Valley fever is currently endemic. This could allow public health agencies to
154 improve surveillance programs and help decrease the time to patient diagnosis. The incidence
155 database also provides a starting point for predicting how climate change will modify the
156 location and extent of endemic areas.

157 The goal of our work was to create a model that describes the area in the US currently
158 endemic to Valley fever and then to use this model to predict how the endemic area may shift in
159 response to climate change. First, we used established relationships between climate and the
160 spatial distribution of Valley fever incidence to create a climate-constrained niche model that
161 predicts the contemporary pattern of Valley fever endemicity. Then, we used our niche model
162 with climate projections from Earth system models to analyze where the climate limits are lifted
163 in the future, potentially allowing the area to become endemic to Valley fever. A secondary goal
164 of our work is to estimate future Valley fever incidence and the number of people who may
165 contract this disease. We report future estimates of the endemic area and potential changes in
166 incidence for the years 2035, 2065, and 2095 under both moderate and high climate warming
167 scenarios. We also examine the compounding effect of climate change and increases in human
168 population on the number of people living in the endemic region and number of potential Valley
169 fever cases. This is the first quantitative projection for the US of how climate change may affect
170 Valley fever. Our predictive model of the endemic area to Valley fever and estimate of future
171 disease burden may provide guidance to public health officials as to where increased Valley
172 fever surveillance and education may improve health outcomes.

173

174 **Methods**

175 ***Valley fever incidence data***

176 To create our models of endemic area and incidence, we used a previously compiled
177 dataset of Valley fever cases for the southwestern US (Gorris et al., 2018). This dataset included
178 monthly, county-level Valley fever cases from 2000–2015 from Arizona, California, Nevada,
179 New Mexico, and Utah. We calculated Valley fever incidence for each county using 2000–2015
180 intercensal population estimates from the US Census Bureau (U.S. Census Bureau, 2011; 2016).
181 We performed our analysis at the county-level, which was the highest resolution available from
182 the state health agencies for the de-identified, aggregated case data.
183
184 ***Current and future projections of climate***
185 We focused our analyses on two main climate drivers that influence the presence of
186 *Coccidioides* ssp. in the environment: temperature and precipitation. We gathered surface air
187 temperature and surface precipitation data for years 2000–2015 to compare directly with Valley
188 fever incidence. For both climate variables, we used 4 km gridded products from the
189 Precipitation-elevation Regressions on Independent Slopes Model (PRISM; Daly et al., 2008).
190 To compare county-level Valley fever incidence data with climate data, we calculated county-
191 level climate averages by spatially averaging the gridded PRISM climate data within each county
192 using QGIS (https://www.qgis.org). We obtained county shapefiles from the US Census Bureau
193 (https://www.census.gov/geo/maps-data/data/tiger-line.html).
194 In previous work, we found a significant, positive nonlinear relationship between county-
195 level mean annual temperature and Valley fever incidence, and a significant, nonlinear inverse
196 relationship between mean annual precipitation and incidence throughout the southwestern US
197 (Figure 1a–b; Gorris et al., 2018). We previously analyzed a suite of climate variables and found
198 that mean annual temperature, mean annual precipitation, mean annual soil moisture, surface

dust concentration, and cropland area had significant relationships with the spatial distribution of Valley fever incidence in the southwestern US (Gorris et al., 2018). We chose to use precipitation here instead of soil moisture for mapping the spatial extent of Valley fever because of large model-to-model differences in the representation of the processes regulating soil moisture content in Coupled Model Intercomparison Project Phase 5 (CMIP5) models. We did not include dust or cropland area because of the ineffectiveness of these variables in constraining Valley fever endemic areas at the continental scale of the contiguous US (data not shown). Analysis of these data show that counties with higher levels of mean annual Valley fever incidence have a hot and dry contemporary climate (Figure 1c).

For future climate projections, we used output of monthly surface air temperature (variable 'tas') and surface precipitation (variable 'pr') from 30 Earth system models from the Bias-Corrected Spatially Downscaled (BCSD) CMIP5 Climate Projections archive (Table SI1; available at https://gdo-dcp.ucllnl.org/downscaled_cmip_projections/; Maurer et al., 2007; Reclamation, 2013). The CMIP5 model simulations were used extensively in the Intergovernmental Panel on Climate Change 5th Assessment Report (Stocker et al., 2013; Taylor et al., 2012). We analyzed data for representative concentration pathway 4.5 (RCP4.5), a moderate fossil fuel emissions and warming scenario in which emissions peak in the mid-21st century and decrease thereafter, and RCP8.5, a high fossil fuel emissions and warming scenario in which emissions increase continuously through the 21st century (Moss et al., 2010). We calculated a mean annual temperature for our analyses by averaging the raw, gridded monthly temperatures and we calculated a mean annual precipitation by taking the sum of monthly precipitation for each year, separately for each of the 30 models.

To estimate future climate, we combined information from the CMIP5 simulations with contemporary climate observations from PRISM. We first selected a baseline period of 2007 (averaging across the years 2000–2015) to match the period of available Valley fever case data. We averaged the raw, gridded CMIP5 output to calculate future mean annual temperature and precipitation for 2035 (the average of years 2030–2040), 2065 (the average of years 2060–2070), and 2095 (the average of years 2090–2100). We used 11-year averages to reduce (but not eliminate) the uncertainty associated with low-frequency internal variability that can make it difficult to detect or quantify trends from anthropogenic forcing (Deser et al., 2012). Next, we spatially averaged these climate projections to the county-level. We then calculated climate anomalies as the difference between each of these future time periods and our baseline period for each county, separately for each CMIP5 model. For mean annual temperature, we calculated the absolute difference between our baseline and each future time period. For mean annual precipitation, we calculated the percent change between the baseline and each future time period. We created climate projections by adding the CMIP5 climate anomalies to our 2007 baseline PRISM data. We averaged the climate anomalies from the 30 CMIP5 simulations to create a multi-model mean climate projection that we added to our 2007 baseline PRISM data; we used this multi-model mean to create our main projections of Valley fever endemicity.

To provide an estimate of the uncertainty in our multi-model mean, we calculated the standard deviation across the 30 CMIP5 simulations for each Valley fever statistic. As another measure of climate projection uncertainty, we report individual model projections of the number of counties endemic to Valley fever in 2095 for both RCP4.5 and RCP8.5 climate scenarios in Table S1. We further used the individual CMIP5 simulations to quantify the level of agreement

among models that each county will become endemic to Valley fever for both the RCP4.5 and RCP8.5 scenarios and report this uncertainty metric in map form.

Our climate projections show the highest warming in the north-central contiguous US and relatively high levels of warming throughout the northern US and Rocky Mountains (Figure 2a–c; Figure S1). Mean annual temperatures are predicted to increase for the RCP8.5 climate scenario by 3.1°C to 6.0°C by the end of the 21st century. Mean annual precipitation is predicted to increase across the Pacific Northwest and in the eastern US, but decrease in the south-central and southwestern US (Figure 2d–f; Figure S2). Both the increase in temperature and changes in precipitation are larger for the RCP8.5 climate scenario than for the RCP4.5 climate scenario (Figure S1; Figure S2).

Climate niche modeling of current and future Valley fever endemic regions

We used the observed relationships between mean annual Valley fever incidence and both mean annual temperature and precipitation to map regions endemic to Valley fever. First, we selected a minimum level of mean annual Valley fever incidence (averaged from 2000–2015) to designate that a county was endemic by comparing our Valley fever incidence data against the CDC endemicity map. We found there were large variations in the mean annual incidence between the three CDC definitions of endemicity: counties considered “highly” endemic by the CDC had mean annual Valley fever incidence between 21.3 and 158.4 cases per 100,000 population per year. Counties considered “established” endemic had between 0.7 and 94.5 cases per 100,000 population per year. Counties considered “suspected” endemic had between 0.0 and 31.8 cases per 100,000 population per year.

Taking these large variations into account, we selected a conservative level of mean annual incidence to define a county as endemic, which we defined as meeting or exceeding 10 cases per 100,000 population per year. This definition included all the counties the CDC defined as "highly" endemic (5/5), over half the counties the CDC described as "established" endemic (16/28), and one county the CDC described as "suspected" endemic (1/44; San Luis Obispo, CA; mean annual incidence of 31.8 cases per 100,000 population).

Then, we examined the mean annual temperature and precipitation for the counties we defined as endemic. For temperature, all of the counties we defined as endemic have a mean annual temperature above 10.7°C (Figure 1). For precipitation, all of the counties we defined as endemic have mean annual precipitation less than 600 mm/yr. We used these two thresholds together to create a climate-constrained niche model which describe the climate necessary for Valley fever endemicity. Our niche model identifies a county as endemic if that county has both a mean annual temperature greater than or equal to 10.7°C and mean annual precipitation less than or equal to 600 mm/yr (Figure 1c).

We applied our climate-constrained niche model to the entire US to estimate the areas which may currently be endemic to Valley fever. Then, we used our climate projections for both the RCP4.5 and RCP8.5 scenarios as input to estimate the areas that may become endemic to Valley fever in years 2035, 2065, and 2095.

We attempted different optimizations of our incidence and climate thresholds to improve the accuracy of our map in comparison to the CDC map. When we apply our climate-constrained niche model to the US, we acknowledge there may be differences between the area we defined as endemic and the area the CDC defines as endemic since the basis for the CDC map is over 65

years old (Edwards & Palmer, 1957). Moreover, Valley fever incidence varies widely for counties within each of the three classes of endemicity defined by the CDC.

As a sensitivity analysis to complement our climate-constrained niche model, we ran the ecological niche model Maxent (R package 'dismo' version 1.1-4 and Maxent version 3.3.3k; Phillips et al., 2006). We trained our model by defining occurrence points as the counties that met our definition of endemicity (10 cases per 100,000 population per year; n = 23). All other counties were considered background points (n = 3085). We ran our models with default configurations, so all feature types were possible. We ran two scenarios with Maxent: one with the PRISM baseline mean annual temperature and mean annual precipitation as explanatory variables and a second with the PRISM mean January temperature, mean July temperature, and mean annual precipitation as explanatory variables. The output of Maxent is a relative environmental suitability measure, ranging from zero to one, where one describes an environment most similar to the training dataset. To identify a county-level endemicity threshold, we optimized the environmental suitability variable to attain the highest accuracy when compared to the CDC endemicity map (comprised of all three CDC endemicity classes; Table S2). Counties at or above this suitability threshold were considered endemic. After this optimization, the two-variable Maxent model has an accuracy of 96.3% and the three-variable Maxent model has an accuracy of 96.8%. As described below, we compared the areas identified as endemic to Valley fever by our climate-constrained niche model to the more conservative predictions from the Maxent models as a sensitivity analysis and report the results in Table S2.

Modeling of current and future mean annual Valley fever incidence

We estimated an upper bound of current and future Valley fever incidence for counties our climate-constrained niche model defined as endemic. To do so, we applied a multiple linear quantile regression using iterative reweighted least squares for the 90th percentile (Eq. 1) using the observed relationships between mean annual Valley fever incidence (*VFI*) and mean annual temperature (*T*) and precipitation (*P*) for the endemic counties (red and blue colored counties in Figure 1, n = 78).

$$VFI = \beta_1 T + \beta_2 P$$

$$VFI = (6.57)T + (-0.12)P$$

Our model had a pseudo r-square (not analogous to ordinary least squares r-square) value of 0.29 describing the local fit for our baseline period. We chose to report the 90th percentile estimate as an indicator of potential Valley fever incidence, recognizing there is a wide spread in the incidence among counties that met our climate-constrained niche model thresholds (Figure 1). Some of this spread may be caused by fine-scale variations in agriculture, dust storms, health care infrastructure, epidemiological reporting, and other natural and socioeconomical factors known to influence *Coccidioides* spp. abundance and disease incidence (Gorris et al., 2018; Louie et al., 1999; Tong et al., 2017; Williams et al., 1979). Following a similar approach to our endemicity analysis, we used the climate projections from CMIP5 to estimate future changes in potential Valley fever incidence.

Projections of human population

To isolate the effects that climate change alone may have on the number of people who contract Valley fever, in our main analysis we assumed an invariant human population in the US. However, US population is projected to increase throughout the 21st century (Hauer, 2019),

which may expose more people to *Coccidioides* ssp. and lead to more Valley fever cases. To estimate the combined effect of both climate change and increasing population, we used future projections of human population from the Shared Socioeconomic Pathways (SSPs; Hauer, 2019) to calculate future population levels within the Valley fever endemic region. The county-level human population projections we used take into account age, sex, and race, and were specifically tailored for the US (Hauer, 2019).

The SSPs describe how socioeconomic factors such as population, economic growth, and technological development evolve in the absence of climate change or climate policy (O'Neill et al., 2014). We used both SSP2, a scenario in which there is moderate population growth in the US throughout the 21st century, and SSP5, a scenario in which there is large population growth (O'Neill et al., 2014). Our 2007 (mean of years 2000–2015) baseline US population is 300 M (U.S. Census Bureau, 2011; 2016). By 2095, SSP2 projects the total US population to be 454 M and SSP5 projects it to be 690 M (Hauer, 2019). We examined each SSP population scenario in combination with the RCP4.5 and RCP8.5 climate scenarios.

Results

Estimating the current spatial extent of Valley fever endemicity

We used our climate-constrained niche model to map counties potentially endemic to Valley fever for the 2007 baseline period (mean of years 2000–2015; Figure 3a). Counties where mean annual temperature and mean annual precipitation are suitable for Valley fever endemicity are shown in magenta. Counties with suitable temperature but unsuitable precipitation are shown in red. Likewise, counties with suitable precipitation but unsuitable temperature are shown in blue. Counties where both temperature and precipitation are unfavorable are shown in white.

355 This analysis reveals that precipitation limits the area endemic to Valley fever to the north along
356 the coast of the Pacific Northwest and to the east across eastern Texas, Oklahoma, and Kansas,
357 whereas temperature limits the northern range of Valley fever endemicity in many interior
358 western states.

359 Using our climate niche model, we estimate 217 counties may currently be endemic to
360 Valley fever. These counties span 12 states–Arizona, California, Colorado, Idaho, Kansas,
361 Nebraska, Nevada, New Mexico, Oklahoma, Texas, Utah, and Washington State. Using the 2007
362 baseline county population estimate, approximately 47.5 M people live within this endemic
363 region (U.S. Census Bureau, 2016).

364 The niche model predicts a spatial pattern of endemicity that is broadly similar to the map
365 produced by the CDC but with several notable differences (Figure 3b). Of the 170 counties
366 identified by the CDC as endemic, the niche model classifies 110 counties as potentially
367 endemic. Of the 60 counties not classified as endemic by our model but identified by the CDC,
368 many are located in southwestern Utah, northwestern New Mexico, and southcentral Texas.
369 Compared to the CDC map, our model also omits a few counties that previously experienced
370 localized outbreaks of Valley fever. These outbreaks include cases contracted in Dinosaur
371 National Monument and Duchesne County in Utah (Peterson et al., 2004), where *Coccidioides*
372 spp. is thought to survive in isolated areas with high soil temperatures, and cases associated with
373 archeological sites in northern California in Tehama and Butte Counties (Werner & Pappagianis,
374 1973; Werner et al., 1972).

375 Our niche model predicts 107 counties as endemic that the CDC model did not identify as
376 endemic. The niche model predicts endemic areas extend farther north throughout the Great
377 Plains and Central Valley of California. These areas include several states that are absent from

the CDC map, including Colorado, Idaho, Kansas, Nebraska, and Oklahoma. The model identifies the two most populous counties in Idaho–Ada and Canyon County–as potentially endemic, including the city of Boise (U.S. Census Bureau, 2016).

One striking similarity between our model estimate and the CDC map is the identification of endemicity in three counties in southeastern Washington State, originally thought to be well outside the endemic region. These counties were recently added to the CDC map after an outbreak of Valley fever cases was reported in 2013 (Marsden-Haug et al., 2012). Since then, *C. immits* has been extracted from Washington State soils (Litvintseva et al., 2014).

Considering the CDC endemic map as truth, our model identifies 2831 counties in the US as true negatives (TN; non-endemic), 110 counties as true positive (TP; endemic), 107 counties as false positives (FP), and 60 counties as false negatives (FN). This corresponds to a 94.6% accuracy rate ([TP+TN]/total) for predicting endemic counties in the US (a 5.4% error rate) and a 64.7% recall rate (TP/[TP+FN]).

The Maxent ecological niche models that we ran as a sensitivity analysis produces similar, but more conservative patterns of contemporary endemicity when compared to our climate-constrained niche model. Both the two-variable and three-variable Maxent models have higher accuracy rates (96.3% and 96.8%, respectively; Table S2). However, the two-variable Maxent model considerably underestimates the number of endemic counties compared to the CDC map, with a 37.6% recall rate; it yields more false negatives (106) and fewer true positives (64) when compared to the climate-constrained niche model. The relative contributions of the environmental variables in the two-variable Maxent model are 80% for mean annual precipitation and 20% for mean annual temperature, highlighting the importance of precipitation in structuring contemporary areas of endemicity. The three-variable Maxent model performs

401 better than the two-variable Maxent model, but again yields more false negatives (79) and fewer
402 true positives (91) compared to the climate-constrained niche model. The relative contributions
403 of variables in the three-variable model are 75% for mean annual precipitation, 25% for mean
404 annual January temperature, and less than 0.1% for mean annual July temperature, which again
405 demonstrates the importance of precipitation and suggests winter temperatures may be more
406 important than summer temperatures in structuring the spatial pattern of endemicity.
407 Overall, our simple, two variable climate-constrained niche model provides a reasonable
408 regional-scale depiction of the area endemic to Valley fever. Other factors such as soil
409 characteristics and competition among microorganisms may further refine where *Coccidioides*
410 spp. is present on finer spatial scales. Additionally, *Coccidioides* spp. may be able to adapt to
411 different soil environments (Colson et al., 2017). Recognizing that many additional processes
412 contribute to *Coccidioides* spp. abundance and disease dynamics at finer spatial scales, our
413 model may enable preliminary exploration of climate change impacts on areas affected by Valley
414 fever throughout the 21st century.
415
416 ***Estimating the future spatial extent of Valley fever endemic regions***
417 We applied our climate-constrained niche model to identify counties that may become
418 endemic to Valley fever in the future for the moderate (RCP4.5) and high (RCP8.5) climate
419 warming scenarios. Over time, the area of climate-constrained endemicity is predicted to expand
420 northward, most notably throughout the Great Plains and in the rain shadows of the Sierra
421 Nevada and Rocky Mountain Ranges (Figure 4; Figure S3). For the high climate warming
422 scenario (RCP8.5), the model predicts by the end of the 21st century the area endemic to Valley
423 fever will more than double (a 113% increase), the number of states with Valley fever

424 endemicity will increase from 12 to 17, the number of counties with endemicity will increase
425 from 217 to 476, and the number of people living within the endemic region will increase by
426 17% (Figure 5). The smaller relative change in human exposure compared to endemic area is
427 caused by increases in endemicity in many western counties that have relatively low population
428 (and follows our assumption here of an invariant population). For the moderate climate warming
429 scenario (RCP4.5), the model predicts that by the end of the century the expansion of Valley
430 fever endemic area will be considerably smaller than for the RCP8.5 scenario, increasing by only
431 about 46% (Figure S3; Figure 5a). Other Valley fever disease metrics also change more slowly
432 for RCP4.5 (Figure 5b-e). The contrast between the two scenarios highlights the importance of
433 climate change mitigation as a means for limiting the health impacts of Valley fever, especially
434 for more northern states (Table S3).

435 By 2035 for RCP8.5, we predict the climate-constrained range of Valley fever will
436 expand into northern Utah and eastern Colorado. By 2065, southern Idaho, Nebraska,
437 southeastern Montana, and South Dakota will become endemic, and by 2095, Valley fever will
438 enter North Dakota and move farther north in Montana. The Valley fever endemic region will
439 expand northward in dry western states primarily as a consequence of warming that pushes mean
440 annual temperatures above the temperature threshold required for disease establishment. From
441 our baseline time period to 2095 for RCP8.5, 242 counties will become endemic to Valley fever
442 because of warming above the temperature threshold, 20 counties will become endemic because
443 of drying below the precipitation threshold, and 3 counties will become unsuitable for
444 endemicity because of increases in precipitation.

445 Precipitation has a key role in determining whether a county becomes endemic in the
446 future. By 2095 for RCP8.5, most of the western US will have a climate that permits Valley

447 fever endemicity, except for counties near the central and northern Pacific Coast and counties at
448 higher elevations in mountain ranges. Northern California, western Oregon, and western
449 Washington State will meet the mean annual temperature threshold yet will be shielded from
450 becoming endemic because of high levels of precipitation. The eastward extent of the climate-
451 constrained endemic range across the Great Plains is also limited for contemporary and future
452 periods by precipitation, with a sustained north-south barrier occurring near the 100°W meridian.
453 This axis corresponds to a zonal atmospheric water vapor gradient where dry, continental air
454 from the southwestern US meets moist, warm maritime air from the Gulf of Mexico, creating a
455 sharp increase in moisture availability to the east (Lin, 2007).

456 We calculated the percent of the individual CMIP5 model simulations that are in
457 agreement that each county will have a climate that permits Valley fever endemicity for the
458 RCP4.5 and RCP8.5 scenarios. There is strong model agreement across the majority of the
459 projected endemic region (Figure 6; Figure S4). By 2095 for RCP8.5, some models predict
460 Valley fever will be endemic farther east throughout the Central Plains, even into Minnesota.
461 However, there is still a clear climate control on the eastern boundary of endemicity driven by
462 the moisture gradient along the 100°W meridian. There is also strong agreement that several high
463 elevation counties within the Rocky Mountains, as well as counties along the northern Pacific
464 Coast, will remain outside the zone of endemicity.

465 As a sensitivity analysis, we ran projections of our Maxent ecological niche models for
466 RCP8.5. Both the two-variable and three-variable Maxent models also predict an expansion of
467 areas endemic to Valley fever along the leeside of the Rocky Mountains and in the dry inland
468 areas of the Pacific Northwest including southeastern Washington State. By 2095 for RCP8.5,
469 the two-variable Maxent model identifies 15 states will have a climate that permits endemicity

and the three-variable Maxent model identifies 14 states (Table S2). We calculated the relative change in the population living within the Valley fever endemic area to compare across models, not considering changes in human population. Our climate-constrained threshold model predicts the population living within the Valley fever endemic area will increase by 6% in year 2035, by 16% in 2065, and by 17% in 2095. Similarly, the two-variable Maxent model predicts a 5% increase in 2035, a 12% increase in 2065, and an 18% increase by 2095. Projections using the three-variable Maxent model show similar changes and yield a 16% increase in the population living within the Valley fever endemic area by 2095. Although the Maxent models are more conservative in estimating the area endemic to Valley fever for the contemporary period, the projected pattern of Valley fever expansion is broadly consistent across all three models. The three-variable Maxent model that includes both January and July mean annual temperatures as explanatory variables allows us to better represent biological limits on the fitness of *Coccidioides* spp. to inhabit regions that experience exceptionally cold winters or hot summers. This more complex model still yields a pattern of future expansion that is similar to the simpler models that use mean annual climate variables.

Estimating current and future mean annual Valley fever incidence

We estimated an upper bound of Valley fever incidence by performing quantile regression on observed Valley fever incidence and mean annual temperature and precipitation (Figure 7). For our baseline period, our model predicts mean annual Valley fever incidence is likely to be greatest in the extreme southwestern US and southwestern Texas (Figure 7). The model also predicts high incidence in the Central Valley of California. For the baseline period, our model predicts up to 34,460 potential cases of Valley fever within Arizona, California,

493 Nevada, New Mexico, and Utah, compared to approximately 9,500 observed cases per year
494 (CDC, 2018a).

495 We then applied our quantile regression model to future climate projections for both
496 RCP4.5 and RCP8.5. Our model predicts Valley fever potential incidence will increase over time
497 throughout the extreme southwestern US, southern Great Plains, Central Valley of California,
498 and the northwestern US (Figure 7; Figure S5). Using our baseline (invariant) human population
499 estimates, we transformed incidence projections into the number of Valley fever cases (Figure
500 5e). The number of potential cases each year for RCP8.5 is projected to increase by 12% in the
501 year 2035 and by 50% in the year 2095.

502

503 ***Compounding effects of climate change and human population projections on Valley fever***

504 Increasing US population will compound disease impacts caused by climate change. By
505 2095 for RCP8.5 assuming an invariant population, we estimate that the number of people living
506 in the Valley fever endemic area will be 55.5 M (Table 1). When we account for both climate
507 change and increasing population, this number increases by 32% (73.2 M) for the SSP2
508 population scenario and by 44% (80.1 M) for the SSP5 population scenario. In concert, the
509 number of potential Valley fever cases will increase by the same percent. The compounding
510 effect between climate change and increasing population in the dry southwestern US highlights
511 the importance of developing more effective approaches for measuring and modeling geospatial
512 patterns of *Coccidioides* spp. abundance and disease risk.

513

514 **Discussion**

515 ***Biogeography of Valley fever expansion***

Our analysis identifies that a primary pathway for Valley fever expansion lies in the rain shadow of the Rocky Mountains. By the end of the 21st century, the climate-constrained area endemic to Valley fever will extend from the southern through the northern Great Plains. This is a predominant region for agriculture, which has a positive correlation with Valley fever incidence (Gorris et al., 2018). Further, climate projections indicate this region will experience an increased risk of drought (Cook et al., 2015). Together, intensifying drought and agriculture may increase the amount of dust loading and thus human exposure to *Coccidioides* spp. It is notable in this context that the Valley fever expansion pathway predicted by our model is through areas affected by the 1930s Dust Bowl (Burnette & Stahle, 2013).

Not all states throughout the Great Plains are required to report Valley fever cases, which may limit our ability to monitor the potential spread of this disease. States in the Great Plains that do report have had minimal cases in recent years (CDC, 2019). There is plausible evidence, however, that *Coccidioides* spp. inhabited this region before. Two buffalo that were radiocarbon dated to be 8500 years old, collected near Milburn, Custer County, Nebraska, showed signs of a fungal infection consistent with Valley fever; the buffalo may have migrated through endemic regions in the south before meeting their demise in Nebraska, or alternatively, the central Great Plains was an endemic region in the past (Morrow, 2006).

Increasing costs of Valley fever for human health

We expect the total number of Valley fever cases and subsequently total cost of disease will increase in concert with the expanding endemic area. Roughly 45% of people with Valley fever are hospitalized (Sondermeyer et al., 2013; Tsang et al., 2010). The estimated median total hospital charge per person in California from 2000–2011 was $55,000 (assuming 2011 USD;

Sondermeyer et al., 2013). Based upon this hospitalization rate, the median total hospital charges (about $58,000 in 2015 USD), and the number of observed cases from 2000–2015 (149,286 cases), we estimate total hospitalization costs are about $244 M per year (2015 USD) for our baseline period. Based on our predicted changes in the relative number of Valley fever cases (and assuming no change in human population) we estimate hospitalization costs due to climate change alone for the RCP8.5 scenario will rise to $274 M per year in 2035, $326 M per year in 2065, and $365 M per year in 2095 (2015 USD). These estimates do not include other costs associated with outpatient care and medications, missed days of work, or childcare (Colby & Ortman, 2014; Sondermeyer et al., 2013; Tsang et al., 2010), nor do they account for the compounding effects of future changes in US population described above.

Improving future projections and sources of uncertainty

Our derived maps of Valley fever endemicity in 2035, 2065, and 2095 describe the disease range constrained solely by future climate. For these areas to become endemic, however, *Coccidioides* spp. needs to physically move into these new areas. This migration may be accomplished by the atmospheric transport of fungal spores in dust or by migration of infected animals, such as rodents (Taylor & Barker, 2019). To reduce uncertainties regarding rates of spread, more work is needed to systematically map the presence of *Coccidioides* spp. in both soils and atmospheric dust throughout the western US.

Our map of the area currently endemic to Valley fever may be helpful in the design of future sampling campaigns to gather occurrence data of *Coccidioides* spp. Once the presence of *Coccidioides* spp. in soils has been systematically mapped, we will be able to build a spatially explicit environmental niche model for *Coccidioides* ssp. directly from environmental

562 surveillance data instead of epidemiological case reports (Miller, 2010; Peterson, 2006) and use
563 this model to determine the response of the fungi to climate change (e.g., Escobar et al., 2016;
564 Romero-Alvarez et al., 2017). As more positive occurrences of *Coccidioides* spp. in the soil are
565 obtained, it will become increasingly critical to simultaneously measure soil properties such as
566 alkalinity, pH, salinity, soil type, soil texture, along with the diversity and presence of other soil
567 microbes to further refine the environmental controls on fungal presence and abundance. High
568 resolution occurrence maps could also help disentangle controls on disease incidence arising
569 from different *Coccidioides* species (Baptista-Rosas et al., 2007; Colson et al., 2017; Lauer,
570 2017) as well as the impacts of heterogeneity in elevation and climate conditions within each
571 county, especially for large counties throughout the western US that span mountainous areas.
572 Concurrently, improved monitoring and reporting of Valley fever cases in states that
573 currently have low or marginal disease incidence would allow for a more accurate delineation of
574 contemporary climate controls. This is most critical for states where current climate conditions
575 permit endemicity (Figure 3), yet the state is not currently reporting, including Colorado, Idaho,
576 Kansas, Oklahoma, and Texas (CDC, 2018a). Proactive surveillance in states where climate does
577 not currently permit endemicity but may in the future will help with monitoring disease spread.
578 Another factor that will likely modulate the number of Valley fever cases in the future is
579 changes in the seasonal and interannual variability of precipitation. Precipitation in California is
580 projected to shift to more intense periods of heavy and extreme rainfall, with moderate to small
581 changes in the overall amount (Polade et al., 2017; Swain et al., 2018). These periods of greater
582 moisture availability may increase fungal growth, while longer and more intense dry periods may
583 enhance dust production and dispersal. In Arizona, summer rainfall brought by the North
584 American monsoon is projected to weaken (Pascale et al., 2017), potentially leading to drier and

585 dustier summers. It's also important to recognize that there is significant low frequency (decadal)
586 internal variability in precipitation in the western US, driven for example by the Pacific Decadal
587 Oscillation (PDO), that may seemingly dampen or amplify the effects of climate change (e.g.,
588 Lehner et al., 2018). In our analysis, variability in precipitation causes some counties to switch
589 back and forth over time in terms of their designation as endemic. For example, the estimated
590 number of California counties endemic to Valley fever for RCP8.5 increases from 28 counties in
591 2035 to 31 counties in 2065, but then decreases to 30 counties in 2095 due to an increase in
592 precipitation in San Francisco County, which was considered endemic in 2065. Evidence of
593 precipitation variability can also be seen in the maps of precipitation change for RCP4.5 (Figure
594 S2), where many areas that are drier in 2035 become wetter again in 2065, contrary to the
595 stronger unidirectional pattern of change associated with anthropogenic forcing in RCP8.5.
596 We used a large set of CMIP5 model simulations to calculate the average projections of
597 climate change for the US. Although some models perform better than others for the US
598 compared to historical observations, the multi-model mean tends to provide a reliable estimate of
599 contemporary surface climate (Sheffield et al., 2013). With improved representation of ocean
600 and atmospheric dynamics and higher spatial resolution, simulations contributed to the 6th
601 Coupled Model Intercomparison Project (CMIP6; Eyring et al., 2016) will likely reduce
602 uncertainties in future projections of temperature and precipitation for the US (Stouffer et al.,
603 2017). The higher quality climate information, along with improved downscaling techniques,
604 will provide better boundary conditions for statistical and mechanistic models predicting changes
605 in Valley fever endemic regions. However, uncertainty in climate projections is only one of the
606 several different types of uncertainty limiting our ability to predict Valley fever endemicity.

Our model draws upon Valley fever incidence data, which implicitly links *Coccidioides* spp. presence with human cases of Valley fever. An important next step is the development of a mechanistic model which separately simulates *Coccidioides* spp. abundance, transmission efficiency, and host heterogeneity as a function of different environmental and human demographic variables. As research on Valley fever and *Coccidioides* spp. continues, additional information such as the possible role of mammals in the fungal life cycle (Taylor & Barker, 2019; Barker, 2018), variations in ecological traits and ecosystems linked to different species of *Coccidioides* (Barker et al., 2012; Colson et al., 2017), and microbial competition (Lauer et al., 2019) will need further consideration for integration into both mechanistic and statistical models of disease incidence. This will be especially important if we learn different *Coccidioides* species have different virulence and tolerances for environmental controls, as this could affect the dispersal of disease and health impacts caused by climate change. As more occurrences of *Coccidioides* spp. in the soil are documented, adding any soil characteristics that limit the presence of the fungi into the model, such as alkalinity, salinity, soil type, and soil texture, may further refine the endemic area (Baptista-Rosas et al., 2007; Colson et al., 2017; Fisher et al., 2007; Maddy, 1957).

Coccidioidomycosis in a global context

Disease surveillance efforts throughout the US and the comprehensive Valley fever case dataset provided the foundation for our study. However, Valley fever is not limited to the US. Our model, as well as the CDC endemicity model, depicts Valley fever endemicity spanning the US-Mexico border. It is well known that *Coccidioides* spp. is present in Mexico; however, there has been minimal disease surveillance within the country (CDC, 2018b; Laniado-Laborin, 2007).

Our future projections indicate the climate-constrained endemic region may also extend north to the US-Canada border by the end of the 21st century, potentially introducing *Coccidioides* spp. to a new country.

We found that the area endemic to Valley fever in the US, as well as the number of cases per year, will increase in response to climate change. Patterns of future change may be similar in other endemic areas within Central and South America. Apart from Mexico, countries that are likely endemic to Valley fever include Guatemala, Honduras, Argentina, Brazil, Paraguay, Bolivia, Venezuela, and Columbia (Colombo et al., 2011; Laniado-Laborin, 2007). International collaboration and Valley fever surveillance in these regions will help delineate the endemic boundaries, provide further information regarding the environmental factors structuring disease presence and incidence, and increase physician awareness (Cat et al., 2019).

Importance of integrating Valley fever into future climate change assessments

The US Global Change Research Program recently suggested climate change may alter the spatial extent and number of Valley fever cases (Crimmins et al., 2016). Our study provides a first estimate to quantitatively describe this change. Furthermore, the Fourth National Climate Assessment report for the US recognized the implications of drought on interannual variability of cases (Ebi et al., 2018). Although the area currently endemic to Valley fever is relatively smaller than other infectious diseases, like West Nile Virus (CDC, 2018c), we expect there may be similar or even larger negative health impacts from the exposure of new communities to Valley fever in response to climate change. In fact, recent mortality rates from Valley fever are similar, if not larger than those reported for West Nile virus. There are approximately 110 deaths per year from West Nile virus in the US (mean 1999–2016; CDC, 2018c) compared to approximately 200

deaths per year from Valley fever (mean 1990–2008; CDC, 2018a). Further, Valley fever cases have increased considerably since 2008, suggesting there may be additional negative impacts from this disease.

Conclusions

We combined a multi-state database of Valley fever incidence observations and climate projections to predict how climate change may influence the endemic area and number of Valley fever cases in the US. Using our climate-constrained niche model, we found the endemic area to Valley fever, as well as the number of cases per year, will increase in response to climate change. As temperatures increase and precipitation patterns change, most of the western US will meet climate thresholds necessary for Valley fever endemicity. Through time, we found the endemic area will expand northward, most notably through the Great Plains. Expansion of the endemic area is suppressed farther east by regional increases in precipitation and the presence of moist air from the Gulf of Mexico. By 2095 for a high climate warming scenario (RCP8.5), our model predicts that 476 counties across 17 states may become endemic to Valley fever. This could result in up to 50% more annual Valley fever cases, before taking into account the compounding effect of future increases in human population. Estimating the regions that may become endemic to Valley fever can mitigate the health effects of this disease, as it will allow health care providers and citizens to prepare in advance. Our research is an example of the necessary bridge between climate science and human health as climate change reshapes areas endemic to infectious diseases.

Acknowledgements

M. E. Gorris is supported by a Department of Defense (DoD), National Defense Science & Engineering Graduate Fellowship (32 CFR 168a). K. K. Treseder acknowledges support from the US NSF (EAR-1411942 and DEB-1457160) and the US Department of Energy, Office of Science, Office of Biological and Environmental Research (BER), under Award Numbers DE-PS02-09ER09-25 and DE-SC001641. C. S. Zender gratefully acknowledges support from the Energy Exascale Earth System Model (E3SM) project, funded by the U.S. Department of Energy, Office of Science, Office of Biological and Environmental Research, from NASA's AIST program, and from the Borrego Valley Endowment Fund. J. T. Randerson acknowledges support from the Gordon and Betty Moore Foundation (GBMF3269), NASA's SMAP, IDS, and CMS research programs, and the RUBISCO Scientific Focus Area that receives funding from the Regional and Global Modeling program within the Biological and Environmental Research division of DOE's Office of Science. We thank the Arizona Department of Health Services, the California Department of Public Health, the New Mexico Department of Health, the Nevada Department of Health and Human Services, and the Utah Department of Health for providing us with Valley fever case data from their respective state health agencies. Valley fever data may be obtained from the affiliated state health agencies. We acknowledge the World Climate Research Programme's Working Group on Coupled Modelling, which is responsible for CMIP, and we thank the climate modeling groups (listed in Table S1 of this paper) for producing and making available their model output. For CMIP, the U.S. Department of Energy's Program for Climate Model Diagnosis and Intercomparison provides coordinating support and led development of software infrastructure in partnership with the Global Organization for Earth System Science Portals. The authors declare no competing financial interests.

699 **References**

700 Ampel, N. M. (2010). What's behind the increasing rates of coccidioidomycosis in
701 Arizona and California?. *Current Infectious Disease Reports*, 12(3), 211–216.
702 https://doi.org/10.1007/s11908-010-0094-3

703 Baptista-Rosas, R. C., Catalán-Dibene, J., Romero-Olivares, A. L., Hinojosa, A.,
704 Cavazos, T., & Riquelme, M. (2012). Molecular detection of *Coccidioides* spp. from
705 environmental samples in Baja California: linking Valley Fever to soil and climate conditions.
706 *Fungal Ecology*, 5(2), 177–190. https://doi.org/10.1016/j.funeco.2011.08.004

707 Baptista-Rosas, R. C., Hinojosa, A., & Riquelme, M. (2007). Ecological niche modeling
708 of *Coccidioides* spp. in western North American deserts. *Annals of the New York Academy of*
709 *Sciences*, 1111(1), 35–46. https://doi.org/10.1196/annals.1406.003

710 Barker, B. M. (2018). Coccidioidomycosis in animals. In S. Seyedmousavi, G. de Hoog,
711 J. Guillot, and P. Verweij (Eds.), *Emerging and Epizootic Fungal Infections in Animals* (pp. 81–
712 114). Springer, Cham. https://doi.org/10.1007/978-3-319-72093-7_4

713 Barker, B. M., Litvintseva, A. P., Riquelme, M., & Vargas-Gastélum, L. (2019).
714 *Coccidioides* ecology and genomics. *Medical Mycology*, 57(Supplement_1), S21–S29.
715 https://doi.org/10.1093/mmy/myy051

716 Barker, B. M., Tabor, J. A., Shubitz, L. F., Perrill, R., & Orbach, M. J. (2012). Detection
717 and phylogenetic analysis of *Coccidioides posadasii* in Arizona soil samples. *Fungal Ecology*,
718 5(2), 163–176. https://doi.org/10.1016/j.funeco.2011.07.010

719 Burnette, D. J., & Stahle, D. W. (2013). Historical perspective on the dust bowl drought
720 in the central United States. *Climatic Change*, 116(3-4), 479–494.
721 https://doi.org/10.1007/s10584-012-0525-2

722 Cat, L. A., Gorris, M. E., Randerson, J. T., Riquelme, M., & Treseder, K. K. (2019).
723 Crossing the Line: Human Disease and Climate Change Across Borders. *Journal of*
724 *Environmental Health*, 81(8), 14–22. https://neha.org/node/60622
725 Catalán-Dibene, J., Johnson, S. M., Eaton, R., Romero-Olivares, A. L., Baptista-Rosas,
726 R. C., Pappagianis, D., & Riquelme, M. (2014). Detection of coccidioidal antibodies in serum of
727 a small rodent community in Baja California, Mexico. *Fungal Biology*, 118(3), 330–339.
728 https://doi.org/10.1016/j.funbio.2014.01.006
729 Centers for Disease Control and Prevention (2017). Valley Fever (Coccidioidomycosis).
730 Retrieved from https://www.cdc.gov/fungal/diseases/coccidioidomycosis/index.html
731 Centers for Disease Control and Prevention (2018a). Valley Fever (Coccidioidomycosis)
732 Statistics. Retrieved from
733 https://www.cdc.gov/fungal/diseases/coccidioidomycosis/statistics.html
734 Centers for Disease Control and Prevention (2018b). Valley Fever Awareness. Retrieved
735 from https://www.cdc.gov/features/valleyfever/index.html
736 Centers for Disease Control and Prevention (2018c). West Nile virus Final Cumulative
737 Maps & Data for 1999–2017. Retrieved from
738 https://www.cdc.gov/westnile/statsmaps/cumMapsData.html
739 Centers for Disease Control and Prevention (2019). Valley fever maps. Retrieved from
740 https://www.cdc.gov/fungal/diseases/coccidioidomycosis/maps.html
741 Chang, D. C., Anderson, S., Wannemuehler, K., Engelthaler, D. M., Erhart, L.,
742 Sunenshine, R. H., et al. (2008). Testing for coccidioidomycosis among patients with
743 community-acquired pneumonia. *Emerging Infectious Diseases*, 14(7), 1053.
744 https://doi.org/10.3201/eid1407.070832

745 Colby, S. L., & Ortman, J. M. (2014). Projections of the Size and Composition of the
746 U.S. Population: 2014 to 2060, Current Population Reports (Report No.: P25-1143) Washington,
747 DC: US Census Bureau.
748 Colombo, A. L., Tobón, A., Restrepo, A., Queiroz-Telles, F., & Nucci, M. (2011).
749 Epidemiology of endemic systemic fungal infections in Latin America. *Medical Mycology*,
750 49(8), 785–798. https://doi.org/10.3109/13693786.2011.577821
751 Colson, A. J., Vredenburgh, L., Guevara, R. E., Rangel, N. P., Kloock, C. T., & Lauer, A.
752 (2017). Large-scale land development, fugitive dust, and increased coccidioidomycosis incidence
753 in the Antelope Valley of California, 1999–2014. *Mycopathologia*, 182(5-6), 439–458.
754 https://doi.org/10.1007/s11046-016-0105-5
755 Comrie, A. C. (2005). Climate factors influencing coccidioidomycosis seasonality and
756 outbreaks. *Environmental Health Perspectives*, 113(6), 688. https://doi.org/10.1289/ehp.7786
757 Cook, B. I., Ault, T. R., & Smerdon, J. E. (2015). Unprecedented 21st century drought
758 risk in the American Southwest and Central Plains. *Science Advances*, 1(1), e1400082.
759 https://doi.org/10.1126/sciadv.1400082
760 Coopersmith, E. J., Bell, J. E., Benedict, K., Shriber, J., McCotter, O., & Cosh, M. H.
761 (2017). Relating coccidioidomycosis (valley fever) incidence to soil moisture conditions.
762 *GeoHealth*, 1(1), 51–63. https://doi.org/10.1002/2016GH000033
763 Crimmins, A., Balbus, J., Gamble, J. L., Beard, C. B., Bell, J. E., Dodgen, D., et al.
764 (Eds.). (2016). *The Impacts of Climate Change on Human Health in the United States: A*
765 *Scientific Assessment*. Washington, DC: US Global Change Research Program.
766 http://dx.doi.org/10.7930/J0R49NQX

767 Daly, C., Halbleib, M., Smith, J. I., Gibson, W. P., Doggett, M. K., Taylor, G. H., et al.
768 (2008). Physiographically sensitive mapping of climatological temperature and precipitation
769 across the conterminous United States. *International Journal of Climatology: A Journal of the*
770 *Royal Meteorological Society*, 28(15), 2031–2064. https://doi.org/10.1002/joc.1688
771 Deser, C., Phillips, A., Bourdette, V., & Teng, H. (2012). Uncertainty in climate change
772 projections: the role of internal variability. *Climate Dynamics*, 38(3-4), 527–546.
773 https://doi.org/10.1007/s00382-010-0977-x
774 Easterling, D. R., Arnold, J. R., Knutson, T., Kunkel, K. E., LeGrande, A. N., Leung, L.
775 R., et al. (2017). Precipitation Change in the United States. In D. J. Wuebbles, D. W. Fahey, K.
776 A. Hibbard, D. J. Dokken, B. C. Stewart, & T. K. Maycock (Eds.), *Climate Science Special*
777 *Report: Fourth National Climate Assessment, Volume I.* Washington, DC: US Global Change
778 Research Program, 207–230. https://doi:10.7930/J0H993CC
779 Ebi, K. L., Balbus, J. M., Luber, G., Bole, A., Crimmins, A., Glass, G., et al. (2018).
780 Human Health. In D. R. Reidmiller, D. R., Avery, C. W., Easterling, D. R., Kunkel, K. E.,
781 Lewis, K. L. M., Maycock, T. K., & Stewart, B. C. (Eds.), *Impacts, Risks, and Adaptation in the*
782 *United States: Fourth National Climate Assessment, Volume II* (pp. 539–571). Washington, DC:
783 U.S. Global Change Research Program. https://doi.org/10.7930/NCA4.2018.CH14
784 Edwards, P. Q., & Palmer, C. E. (1957). Prevalence of sensitivity to coccidioidin, with
785 special reference to specific and nonspecific reactions to coccidioidin and to histoplasmin. *Chest*,
786 31(1), 35–60. https://doi.org/10.1378/chest.31.1.35
787 Escobar, L. E., Romero-Alvarez, D., Leon, R., Lepe-Lopez, M. A., Craft, M. E., Borbor-
788 Cordova, M. J., & Svenning, J. C. (2016). Declining prevalence of disease vectors under climate
789 change. *Scientific Reports*, 6. https://doi.org/10.1038/srep39150

Eyring, V., Bony, S., Meehl, G. A., Senior, C. A., Stevens, B., Stouffer, R. J., & Taylor, K. E. (2016). Overview of the Coupled Model Intercomparison Project Phase 6 (CMIP6) experimental design and organization. *Geoscientific Model Development*, 9(5), 1937–1958. https://doi.org/10.5194/gmd-9-1937-2016

Fisher, F. S., Bultman, M. W., Johnson, S. M., Pappagianis, D., & Zaborsky, E. (2007). *Coccidioides* niches and habitat parameters in the southwestern United States. *Annals of the New York Academy of Sciences*, 1111(1), 47–72. https://doi.org/10.1196/annals.1406.031

Gorris, M. E., Cat, L. A., Zender, C. S., Treseder, K. K., & Randerson, J. T. (2018). Coccidioidomycosis dynamics in relation to climate in the southwestern United States. *GeoHealth*, 2(1), 6–24. https://doi.org/10.1002/2017GH000095

Greene, D. R., Koenig, G., Fisher, M. C., & Taylor, J. W. (2000). Soil isolation and molecular identification of *Coccidioides immitis*. *Mycologia*, 92(3), 406–410. https://doi.org/10.2307/3761498

Hauer, M. E. (2019). Population projections for US counties by age, sex, and race controlled to shared socioeconomic pathway. *Scientific Data*, 6, 190005. https://doi.org/10.1038/sdata.2019.5

Hayhoe, K., Wuebbles, D. J., Easterling, D. R., Fahey, D. W., Doherty, S., Kossin, J., et al. (2018) Our Changing Climate. In D. R. Reidmiller, C. W. Avery, D. R. Easterling, K. E. Kunkel, K. L. M. Lewis, T. K. Maycock, & B. C. Stewart (Eds.), *Impacts, Risks, and Adaptation in the United States: Fourth National Climate Assessment, Volume II* (pp. 72–144). Washington, DC: U.S. Global Change Research Program. https://doi:10.7930/NCA4.2018.CH2

811 Jones, J. M., Koski, L., Khan, M., Brady, S., Sunenshine, R., & Komatsu, K.K. (2017).
812 Coccidioidomycosis: An underreported cause of death—Arizona, 2008–2013. *Medical*
813 *Mycology*, 56(2), 172–179. https://doi.org/10.1093/mmy/myx041
814 Kolivras, K. N., & Comrie, A. C. (2003). Modeling valley fever (coccidioidomycosis)
815 incidence on the basis of climate conditions. *International Journal of Biometeorology*, 47(2), 87–
816 101. https://doi.org/10.1007/s00484-002-0155-x
817 Komatsu, K., Vaz, V., McRill, C., & Colman, T. (2003). Increase in coccidioidomycosis-
818 Arizona, 1998-2001. *Morbidity and Mortality Weekly Report*, 56(6), 109–112. Retrieved from
819 https://www.cdc.gov/MMWR/preview/mmwrhtml/mm5206a4.htm
820 Laniado-Laborin, R. A. (2007). Expanding understanding of epidemiology of
821 coccidioidomycosis in the Western hemisphere. *Annals of the New York Academy of Sciences*,
822 1111(1), 19–34. https://doi.org/10.1196/annals.1406.004
823 Lauer, A. (2017). Coccidioidomycosis: increasing incidence of an “orphan” disease in
824 response to environmental changes. In C. Hurst (Ed.), *Modeling the Transmission and*
825 *Prevention of Infectious Disease* (Vol. 4, pp. 151–185). Springer, Cham.
826 https://doi.org/10.1007/978-3-319-60616-3_6
827 Lauer, A., Baal, J. D. H., Baal, J. C. H., Verma, M., & Chen, J. M. (2012). Detection of
828 *Coccidioides immitis* in Kern County, California, by multiplex PCR. *Mycologia*, 104(1), 62–69.
829 https://doi.org/10.3852/11-127
830 Lauer, A., Baal, J. D., Mendes, S. D., Casimiro, K. N., Passaglia, A. K., Valenzuela, A.
831 H., & Guibert, G. (2019). Valley fever on the rise—searching for microbial antagonists to the
832 fungal pathogen *Coccidioides immitis*. *Microorganisms*, 7(2), 31–47.
833 https://doi.org/10.3390/microorganisms7020031

Lauer, A., Talamantes, J., Olivares, L. R. C., Medina, L. J., Baal, J. D. H., Casimiro, K., et al. (2014). Combining forces-the use of landsat TM satellite imagery, soil parameter information, and multiplex PCR to detect *Coccidioides immitis* growth sites in Kern County, California. *PloS One*, 9(11), e111921:1–14. https://doi.org/10.1371/journal.pone.0111921

Lehner, F., Deser, C., Simpson, I. R., & Terray, L. (2018). Attributing the U.S. Southwest's recent shift into drier conditions. *Geophysical Research Letters*, 45, 6251–6261. https://doi.org/10.1029/2018GL078312

Lin, Y. 2007. *Mesoscale dynamics* (pp. 413–420). Cambridge University Press. https://doi.org/10.1017/CBO9780511619649

Litvintseva, A. P., Marsden-Haug, N., Hurst, S., Hill, H., Gade, L., Driebe, E. M., et al. (2014). Valley fever: finding new places for an old disease: *Coccidioides immitis* found in Washington State soil associated with recent human infection. *Clinical Infectious Diseases*, 60(1), e1–e3. https://doi.org/10.1093/cid/ciu681

Louie, L., Ng, S., Hajjeh, R., Johnson, R., Vugia, D., Werner, S. B., et al. (1999). Influence of host genetics on the severity of coccidioidomycosis. *Emerging Infectious Diseases*, 5(5), 672–680. https://doi.org/10.3201/eid0505.990508

Maddy, K. T. (1957). Ecological factors of the geographic distribution of *Coccidioides immitis*. *Journal of the American Veterinary Medical Association*, 130(11). 475–476.

Marsden-Haug, N., Goldoft, M., Ralston, C., Limaye, A. P., Chua, J., Hill, H., et al. (2012). Coccidioidomycosis acquired in Washington state. *Clinical Infectious Diseases*, 56(6), 847–850. https://doi.org/10.1093/cid/cis1028

Maurer, E. P., Brekke, L., Pruitt, T., & Duffy, P. B. (2007). Fine-resolution climate projections enhance regional climate change impact studies. *Eos, Transactions American Geophysical Union*, 88(47), 504–504. https://doi.org/10.1029/2007EO470006

Miller, J. (2010). Species distribution modeling. *Geography Compass*, 4(6), 490–509. https://doi.org/10.1111/j.1749-8198.2010.00351.x

Morrow, W. (2006). Holocene coccidioidomycosis: Valley Fever in early Holocene bison (*Bison antiquus*). *Mycologia*, 98(5), 669–677.

Moss, R. H., Edmonds, J. A., Hibbard, K. A., Manning, M. R., Rose, S. K., Van Vuuren, D. P., et al. (2010). The next generation of scenarios for climate change research and assessment. *Nature*, 463, 747–756. https://doi.org/10.1038/nature08823

O'Neill, B. C., Kriegler, E., Riahi, K., Ebi, K. L., Hallegatte, S., Carter, T. R., et al. (2014). A new scenario framework for climate change research: the concept of shared socioeconomic pathways. *Climatic Change*, 122(3), 387–400. https://doi.org/10.1007/s10584-013-0905-2

Park, B. J., Sigel, K., Vaz, V., Komatsu, K., McRill, C., Phelan, M., et al. (2005). An epidemic of coccidioidomycosis in Arizona associated with climatic changes, 1998–2001. *The Journal of Infectious Diseases*, 191(11), 1981–1987. https://doi.org/10.1086/430092

Pascale, S., Boos, W. R., Bordoni, S., Delworth, T. L., Kapnick, S. B., Murakami, H., et al. (2017). Weakening of the North American monsoon with global warming. *Nature Climate Change*, 7(11), 806. https://doi.org/10.1038/NCLIMATE3412

Peterson, A. T. (2006). Ecologic niche modeling and spatial patterns of disease transmission. *Emerging Infectious Diseases*, 12(12), 1822–1826. https://doi.org/10.3201/eid1212.060373

878 Petersen, L. R., Marshall, S. L., Barton, C., Hajjeh, R. A., Lindsley, M. D., Warnock, D.
879 W., et al. (2004). Coccidioidomycosis among workers at an archeological site, northeastern Utah.
880 *Emerging Infectious Diseases*, 10(4), 637–642. https://doi.org/10.3201/eid1004.030446
881 Phillips, S. J., Anderson, R. P., & Schapire, R. E. (2006). Maximum entropy modeling of
882 species geographic distributions. *Ecological Modelling*, 190(3–4), 231–259.
883 https://doi.org/10.1016/j.ecolmodel.2005.03.026
884 Polade, S. D., Gershunov, A., Cayan, D. R., Dettinger, M. D., & Pierce, D. W. (2017).
885 Precipitation in a warming world: Assessing projected hydro-climate changes in California and
886 other Mediterranean climate regions. *Scientific Reports*, 7(1), 10783.
887 https://doi.org/10.1038/s41598-017-11285-y
888 Reclamation, 2013. Downscaled CMIP3 and CMIP5 Climate and Hydrology Projections:
889 Release of Downscaled CMIP5 Climate Projections, Comparison with preceding Information,
890 and Summary of User Needs, prepared by the U.S. Department of the Interior, Bureau of
891 Reclamation, Technical Services Center, Denver, Colorado. 47 pp. https://gdo-
892 dcp.ucllnl.org/downscaled_cmip_projections/techmemo/downscaled_climate.pdf
893 Romero-Alvarez, D., Escobar, L. E., Varela, S., Larkin, D. J., & Phelps, N. B. (2017).
894 Forecasting distributions of an aquatic invasive species (*Nitellopsis obtusa*) under future climate
895 scenarios. *PloS One*, 12(7), e0180930:1–24. https://doi.org/10.1371/journal.pone.0180930
896 Sheffield, J., Barrett, A. P., Colle, B., Nelun Fernando, D., Fu, R., Geil, K. L., et al.
897 (2013). North American climate in CMIP5 experiments. Part I: Evaluation of historical
898 simulations of continental and regional climatology. *Journal of Climate*, 26(23), 9209–9245.
899 https://doi.org/10.1175/JCLI-D-12-00592.1

Sondermeyer, G., Lee, L., Gilliss, D., Tabnak, F., & Vugia, D. (2013). Coccidioidomycosis-associated hospitalizations, California, USA, 2000–2011. *Emerging Infectious Diseases*, 19(10), 1590–1597. https://doi.org/10.3201/eid1910.130427

Stewart, R.A., & Meyer, K.F. (1932). Isolation of *Coccidioides immitis* (Stiles) from the soil. *Proceedings of the Society for Experimental Biology and Medicine*, 29(8), 937–938. https://doi.org/10.3181/00379727-29-6159

Stocker, T. F., Qin, D., Plattner, G. K., Tignor, M., Allen, S. K., Boschung, J., et al. (Eds.). (2013). *Intergovernmental Panel on Climate Change. Climate Change 2013: The Physical Science Basis. Contribution of Working Group I to the Fifth Assessment Report of the Intergovernmental Panel on Climate Change.* Cambridge and New York: Cambridge University Press. http://www.ipcc.ch/report/ar5/wg1/

Stouffer, R. J., Eyring, V., Meehl, G. A., Bony, S., Senior, C., Stevens, B., & Taylor, K. E. (2017). CMIP5 scientific gaps and recommendations for CMIP6. *Bulletin of the American Meteorological Society*, 98(1), 95-105. https://doi.org/10.1175/BAMS-D-15-00013.1

Swain, D. L., Langenbrunner, B., Neelin, J. D., & Hall, A. (2018). Increasing precipitation volatility in twenty-first-century California. *Nature Climate Change*, 8(5), 427. https://doi.org/10.1038/s41558-018-0140-y

Talamantes, J., Behseta, S., & Zender, C. S. (2007). Fluctuations in climate and incidence of coccidioidomycosis in Kern County, California. *Annals of the New York Academy of Sciences*, 1111(1), 73–82. https://doi.org/10.1196/annals.1406.028

Tamerius, J. D., & Comrie, A. C. (2011). Coccidioidomycosis incidence in Arizona predicted by seasonal precipitation. *PLoS One*, 6(6), e21009:1–7. https://doi.org/10.1371/journal.pone.0021009

Taylor, J.W., & Barker, B.M. (2019). The endozoan, small-mammal reservoir hypothesis and the life cycle of *Coccidioides* species. *Medical Mycology*, 57(Supplement_1), S16–S20. https://doi.org/10.1093/mmy/myy039

Taylor, K. E., Stouffer, R. J., & Meehl, G. A. (2012). An overview of CMIP5 and the experiment design. *Bulletin of the American Meteorological Society*, 93(4), 485–498. https://doi.org/10.1175/BAMS-D-11-00094.1

Tong, D. Q., Wang, J. X., Gill, T. E., Lei, H., & Wang, B. (2017). Intensified dust storm activity and Valley fever infection in the southwestern United States. *Geophysical Research Letters*, 44(9), 4304–4312. https://doi.org/10.1002/2017GL073524

Tsang, C. A., Anderson, S. M., Imholte, S. B., Erhart, L. M., Chen, S., Park, B. J., et al. (2010). Enhanced surveillance of coccidioidomycosis, Arizona, USA, 2007–2008. *Emerging Infectious Diseases*, *16*(11), 1738–1744. https://doi.org/10.3201/eid1611.100475.

U.S. Census Bureau (2011). Intercensal estimates of the resident population for counties: April 1, 2000 to July 1, 2010. Retrieved from http://www.census.gov/data/tables/time-series/demo/popest/intercensal-2000-2010-counties.html

U.S. Census Bureau (2016). Annual estimates of the resident population: April 1, 2010 to July 1, 2016. Retrieved from https://factfinder.census.gov/faces/tableservices/jsf/pages/productview.xhtml?pid=PEP_2016_PEPANNRES&prodType=table

Vargas-Gastélum, L., Romero-Olivares, A. L., Escalante, A. E., Rocha-Olivares, A., Brizuela, C., & Riquelme, M. (2015). Impact of seasonal changes on fungal diversity of a semi-arid ecosystem revealed by 454 pyrosequencing. *Federation of European Microbiological Societies Microbiology Ecology*, 91(5), fiv044:1–13. https://doi.org/10.1093/femsec/fiv044

946 Werner, S. B., & Pappagianis, D. (1973). Coccidioidomycosis in northern California—an
947 outbreak among archeology students near Red Bluff. *California Medicine*, 119(3), 16–20.
948 Werner, S. B., Pappagianis, D., Heindl, I., & Mickel, A. (1972). An epidemic of
949 coccidioidomycosis among archeology students in northern California. *New England Journal of*
950 *Medicine*, 286(10), 507–512. https://doi.org/10.1056/NEJM197203092861003
951 Wilken, J. A., Sondermeyer, G., Shusterman, D., McNary, J., Vugia, D. J., McDowell,
952 A., et al. (2015). Coccidioidomycosis among workers constructing solar power farms, California,
953 USA, 2011–2014. *Emerging Infectious Diseases*, 21(11), 1997–2005.
954 https://doi.org/10.3201/eid2111.150129
955 Williams, P. L., Sable, D. L., Mendez, P., & Smyth, L. T. (1979). Symptomatic
956 Coccidioidomycosis following a Severe Natural Dust Storm: An Outbreak at the Naval Air
957 Station, Lemoore, Calif. *Chest*, 76(5), 566–570. https://doi.org/10.1378/chest.76.5.566
958 Zender, C. S., & Talamantes, J. (2006). Climate controls on valley fever incidence in
959 Kern County, California. *International Journal of Biometeorology*, 50(3), 174–182.
960 https://doi.org/10.1007/s00484-005-0007-6
961

962 **Table 1.** Compounding effects of climate change and increasing human population on the
963 number of people in millions living in the endemic region for Valley fever in the years 2035,
964 2065, and 2095, relative to our 2007 baseline population estimate of 47.5 M.

	RCP4.5 Climate			RCP8.5 Climate		
	2035	**2065**	**2095**	**2035**	**2065**	**2095**
No change in population (M)	49.9	52.1	52.7	50.1	55.0	55.5
SSP2 population scenario (M)	65.7	68.6	69.7	66.0	72.6	73.2
SSP5 population scenario (M)	71.9	75.0	76.2	72.2	79.4	80.1

965

966

967 **Figure Captions**

968 ***Figure 1.*** Valley fever incidence for counties in the southwestern US (n = 152) as a function of
969 mean annual temperature (a) and mean annual precipitation (b). All counties that have endemic
970 levels of Valley fever incidence (defined as meeting or exceeding 10 or more cases per 100,000
971 population during 2000–2015; n = 23) have a mean annual temperature greater than or equal to
972 10.7°C and a mean annual precipitation level less than or equal to 600 mm/yr. Counties with
973 higher levels of mean annual Valley fever incidence are concurrently hotter and drier (c). We
974 adapted panels a and b of this figure from Gorris et al. (2018) and added the gray lines to indicate
975 the position of the climate thresholds we used to build our climate-constrained niche model.
976 ***Figure 2.*** RCP8.5 climate projections indicate warming throughout the contiguous US with the
977 highest levels occurring in northern states (a–c). Changes in precipitation will vary by region.
978 RCP8.5 projections indicate drying in the southwestern US and south-central Great Plains and
979 wetting across the Pacific Northwest and eastern US (d–f). The difference panels (c, f) are the
980 difference between the 2095 and 2007 maps for each climate variable.
981 ***Figure 3.*** Counties our climate-constrained niche model identify as endemic (with a mean annual
982 temperature greater than or equal to 10.7°C and a mean annual precipitation level less than or
983 equal to 600 mm/yr) are colored in magenta in panel a. There is reasonable agreement between
984 this set of counties and the endemic region identified by the CDC shown in panel b. Counties
985 shown in red in panel a have a mean annual temperature greater than or equal to 10.7°C but
986 unsuitable mean annual precipitation (greater than 600 mm/yr). Counties shown in blue have a
987 mean annual precipitation level less than or equal to 600 mm/yr but unsuitable mean annual
988 temperature (less than 10.7°C). Counties in white our model defines as unsuitable according to
989 both thresholds.

990 ***Figure 4.*** For the RCP8.5 climate change scenario, areas where climate will permit Valley fever
991 endemicity are shown for the years (a) 2035, (b) 2065, and (c) 2095. Areas where mean annual
992 temperature will permit endemicity are shown in red, areas where mean annual precipitation will
993 permit endemicity are shown in blue, and areas where both temperature and precipitation will
994 permit endemicity are shown in magenta, following the color scheme used in Figure 3. The area
995 endemic to Valley fever will extend farther north in future decades, especially in the rain
996 shadows of the Sierra Nevada and Rocky Mountains Ranges. Precipitation will play a key role in
997 determining which areas become endemic through time, as greater rainfall and moisture
998 availability will limit the eastward extent of Valley fever as well as its presence in the Pacific
999 Northwest and in western counties at higher elevations.
1000 ***Figure 5.*** Time series of change in (a) the total area potentially endemic to Valley fever, (b) the
1001 number of endemic states, (c) the number of endemic counties, (d) the number of people living
1002 within endemic regions, and (e) the estimated number of annual cases from 2007 to 2095 for
1003 both RCP8.5 and RCP4.5 climate scenarios. The shaded areas are the standard deviation
1004 describing variation among the 30 CMIP5 Earth system models used in our analyses.
1005 ***Figure 6***. There is strong model agreement throughout the majority of the area we estimate as
1006 endemic to Valley fever for the RCP8.5 climate scenario in years (a) 2035, (b) 2065, and (c)
1007 2095. The model agreement shows a measure of uncertainty for the counties along the edge of
1008 the endemic area. Some models predict the endemic range in 2095 will expand into counties as
1009 far east as western Minnesota. Percent model agreement was calculated as the number of
1010 individual CMIP5 models that predict the county will have a climate that permits endemicity,
1011 divided by the total number of models (n = 30), as projected by the climate-constrained niche
1012 model.

1013 ***Figure 7.*** We estimated an upper bound of future Valley fever incidence using a 90th percentile
1014 regression model for (a) our 2007 baseline period, (b) 2035, (c) 2065, and (d) 2095 for RCP8.5.
1015 Over time, our model predicts Valley fever incidence will increase throughout the extreme
1016 southwestern US and the southern Great Plains. Incidence will also increase throughout the
1017 Central Valley of California and in the northwestern US.

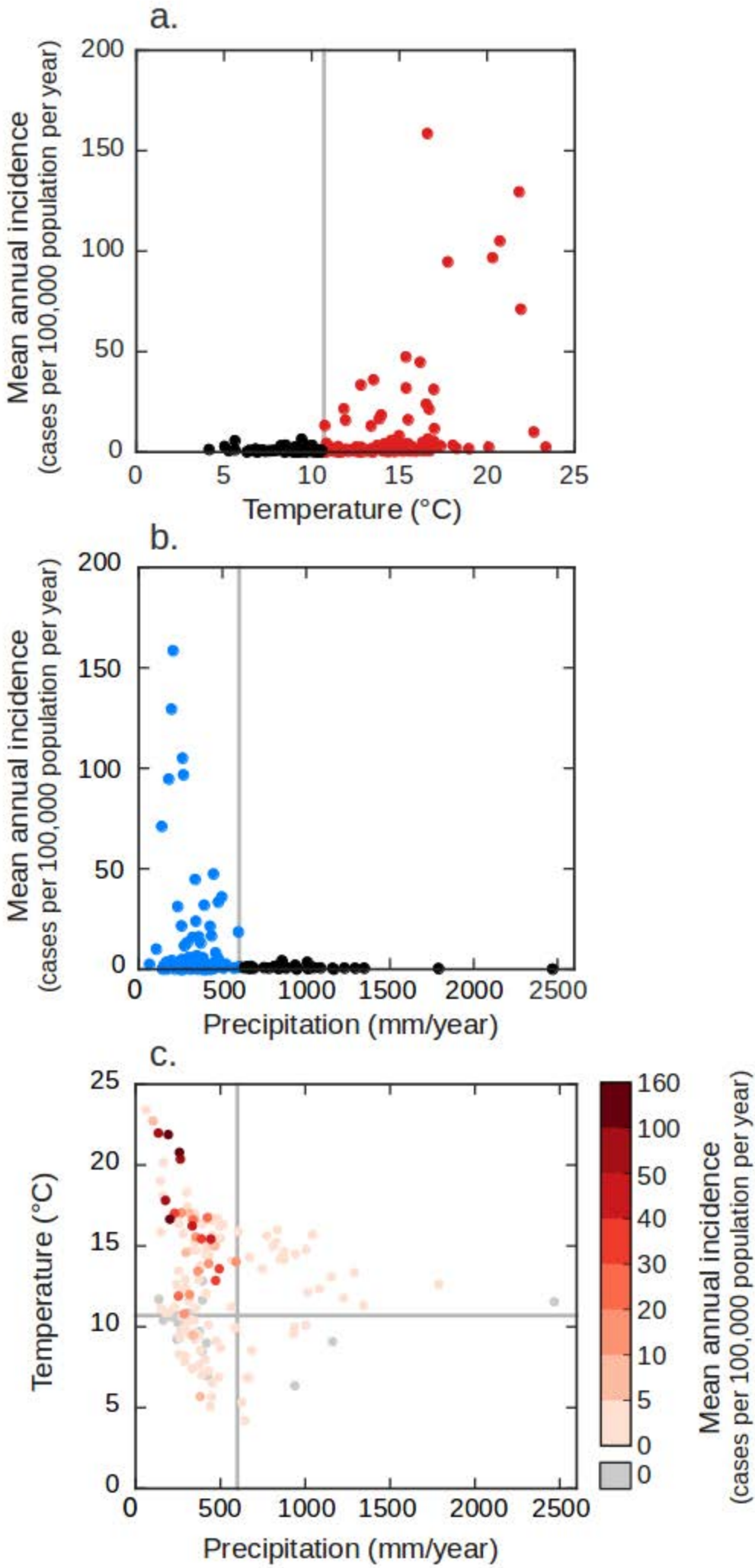
a.
Mean annual incidence
(cases per 100,000 population per year)
200
150
100
50
0
0
5
10
15
20
25
Temperature (°C)
b.
Mean annual incidence
(cases per 100,000 population per year)
200
150
100
50
0
0
500
1000
1500
2000
2500
Precipitation (mm/year)
c.
Temperature (°C)
25
20
15
10
5
0
0
500
1000
1500
2000
2500
Precipitation (mm/year)
160
100
50
40
30
20
10
5
0
0
Mean annual incidence
(cases per 100,000 population per year)

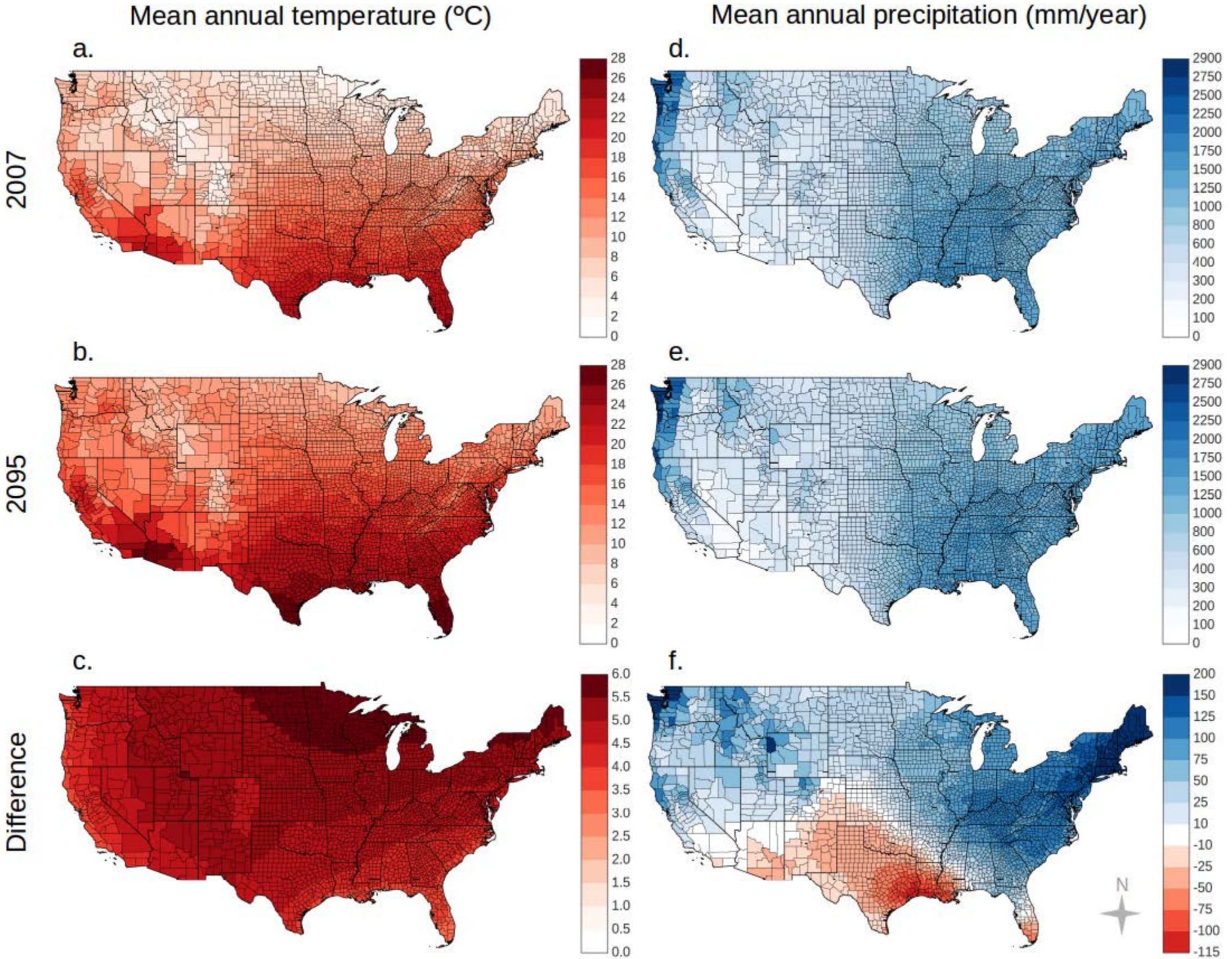
Mean annual temperature (ºC)
Mean annual precipitation (mm/year)
a.
b.
c.
d.
e.
f.
2007
2095
Difference
28 26 24 22 20 18 16 14 12 10 8 6 4 2 0
2900 2750 2500 2250 2000 1750 1500 1250 1000 800 600 400 300 200 100 0
6.0 5.5 5.0 4.5 4.0 3.5 3.0 2.5 2.0 1.5 1.0 0.5 0.0
200 150 125 100 75 50 25 10 -10 -25 -50 -75 -100 -115
N

a. Climate threshold model (2007)

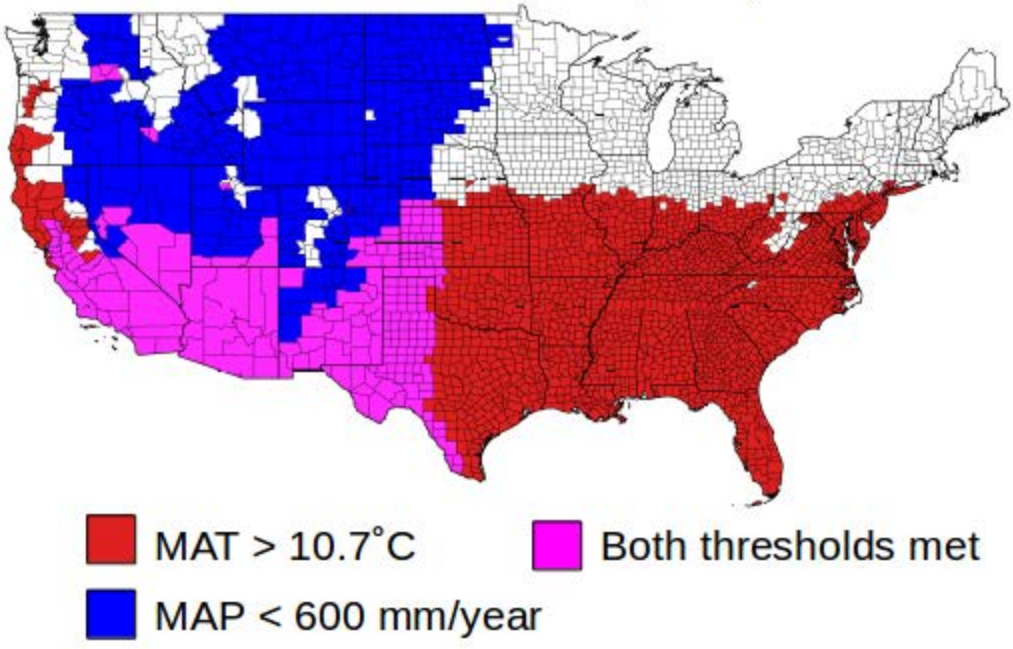

b. CDC

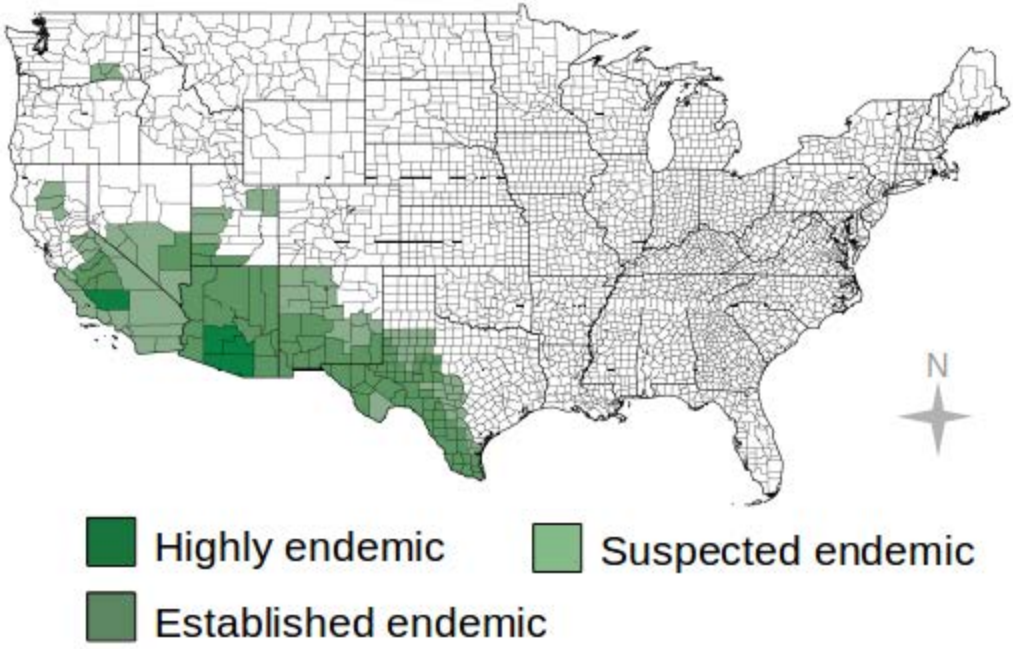

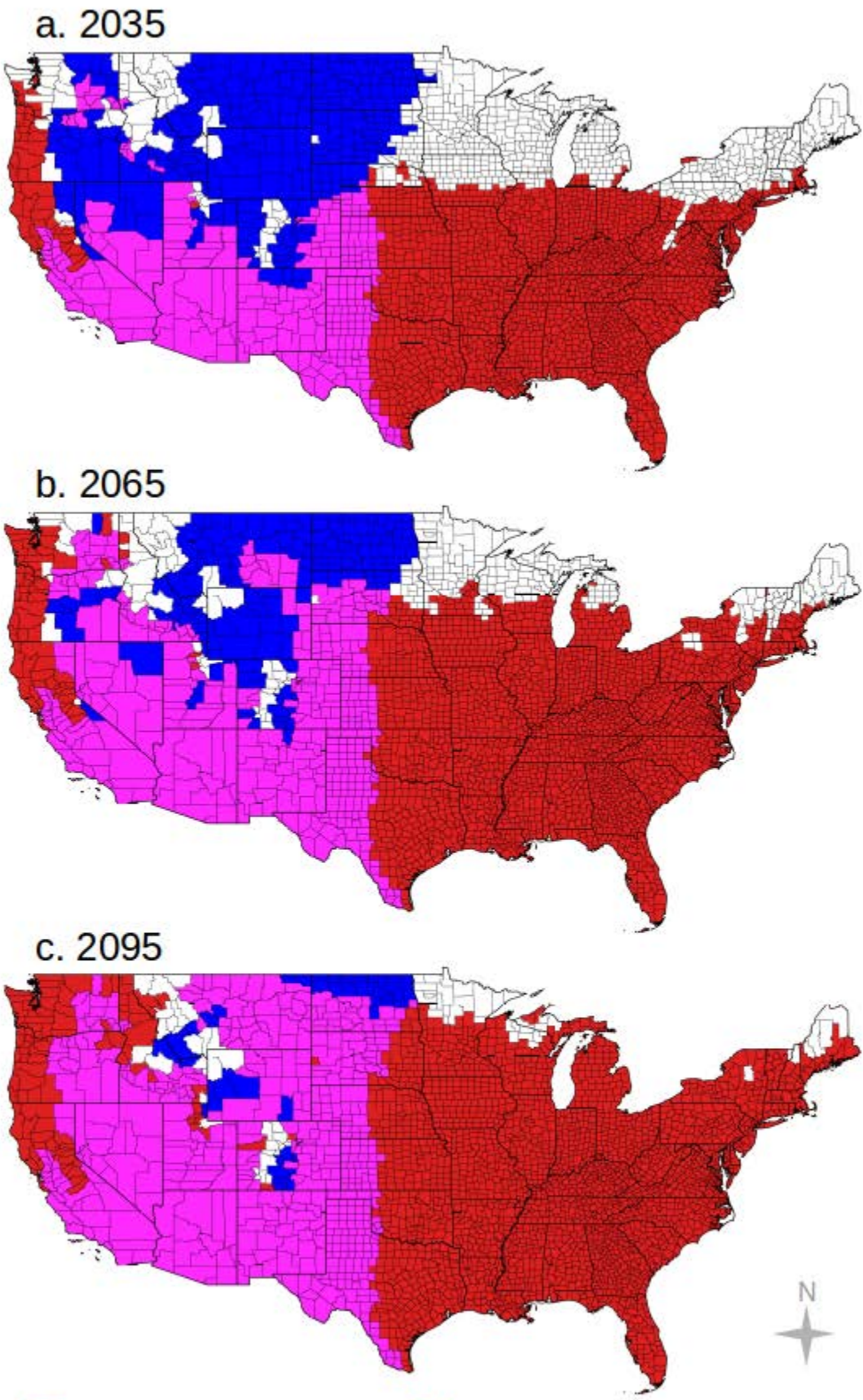
a. 2035
b. 2065
c. 2095
N
MAT > 10.7˚C
Both thresholds met
MAP < 600 mm/year

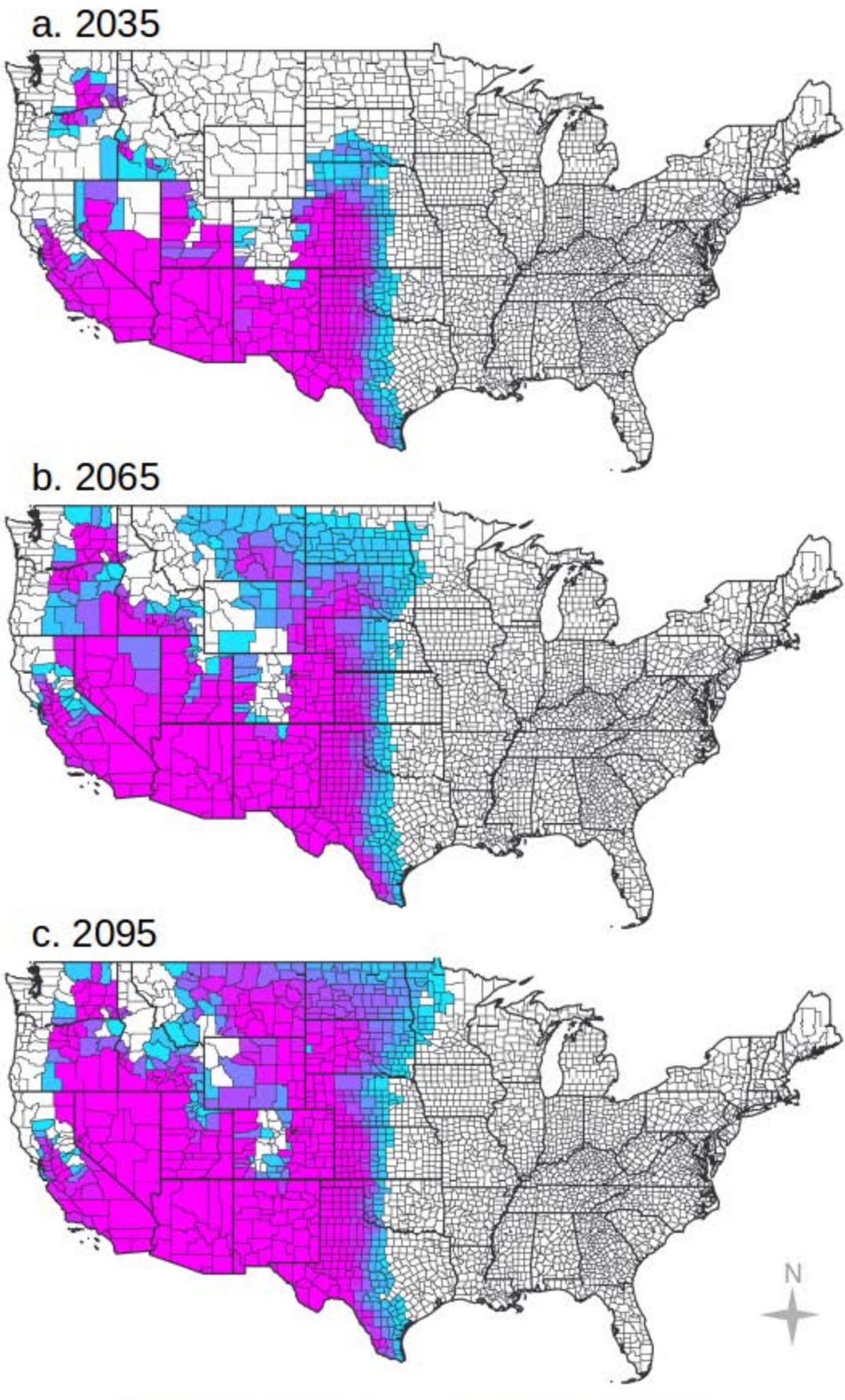
a. 2035
b. 2065
c. 2095
N
0 10 20 30 40 50 60 70 80 90 100
Model agreement (%)

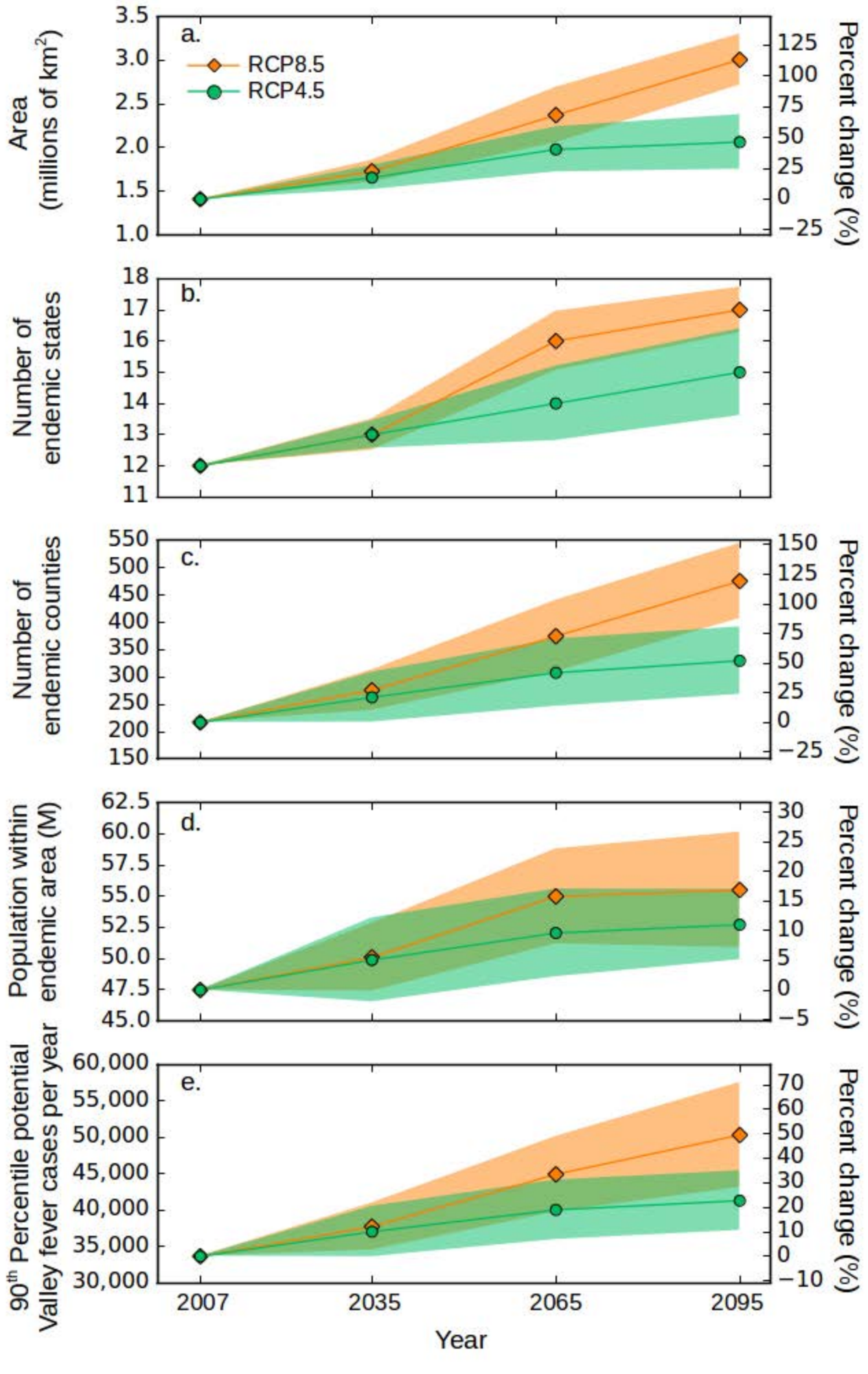
a.
RCP8.5
RCP4.5
Area (millions of km²)
Percent change (%)
b.
Number of endemic states
c.
Number of endemic counties
d.
Population within endemic area (M)
e.
90th Percentile potential Valley fever cases per year
2007
2035
2065
2095
Year

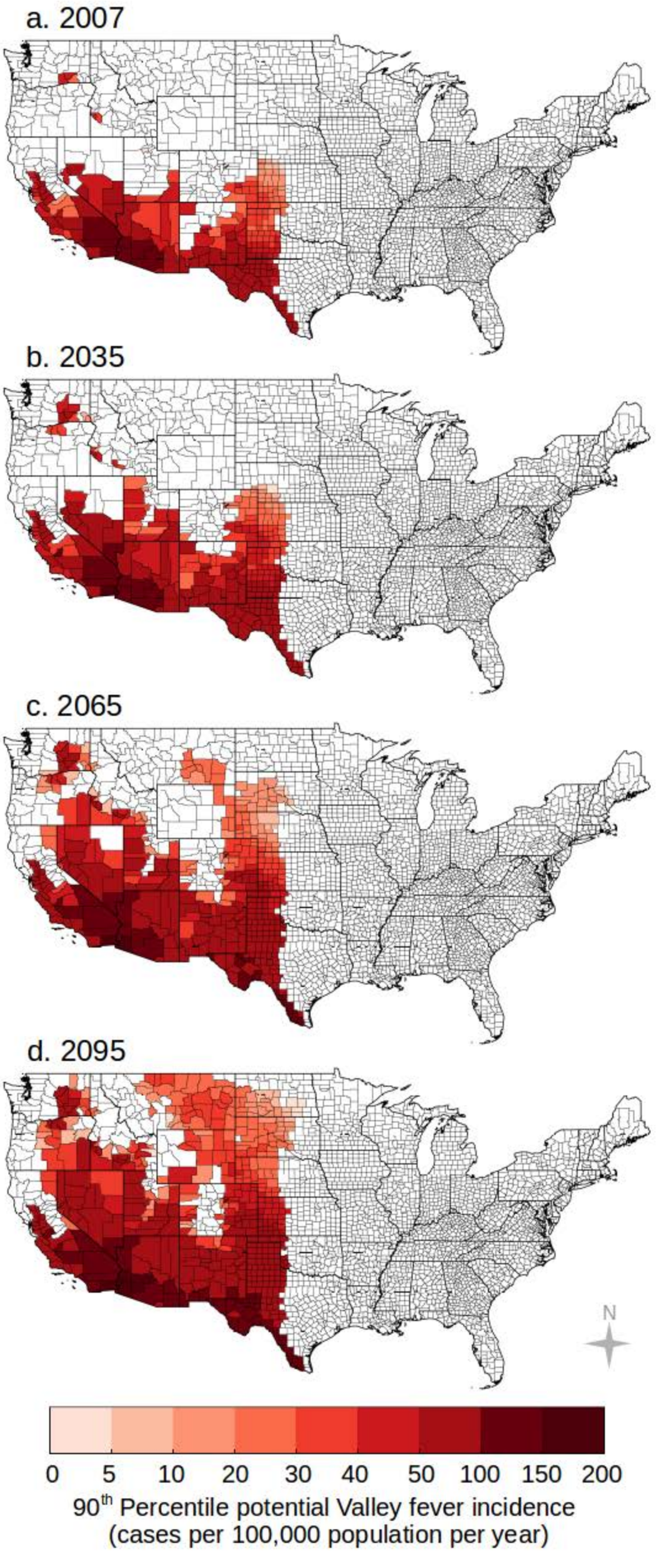
a. 2007
b. 2035
c. 2065
d. 2095
N
0
5
10
20
30
40
50
100
150
200
90th Percentile potential Valley fever incidence
(cases per 100,000 population per year)

RCP4.5

RCP8.5

2035

2065

2095

a.

d.

b.

e.

c.

f.

0 0.5 1.0 1.5 2.0 2.5 3.0 3.5 4.0 4.5 5.0 5.5 6.0

Change in mean annual temperature (°C)

RCP4.5

RCP8.5

2035

2065

2095

a.

b.

c.

d.

e.

f.

-115 -100 -75 -50 -25 -10 10 25 50 75 100 125 150 200

Change in mean annual precipitation (mm/year)

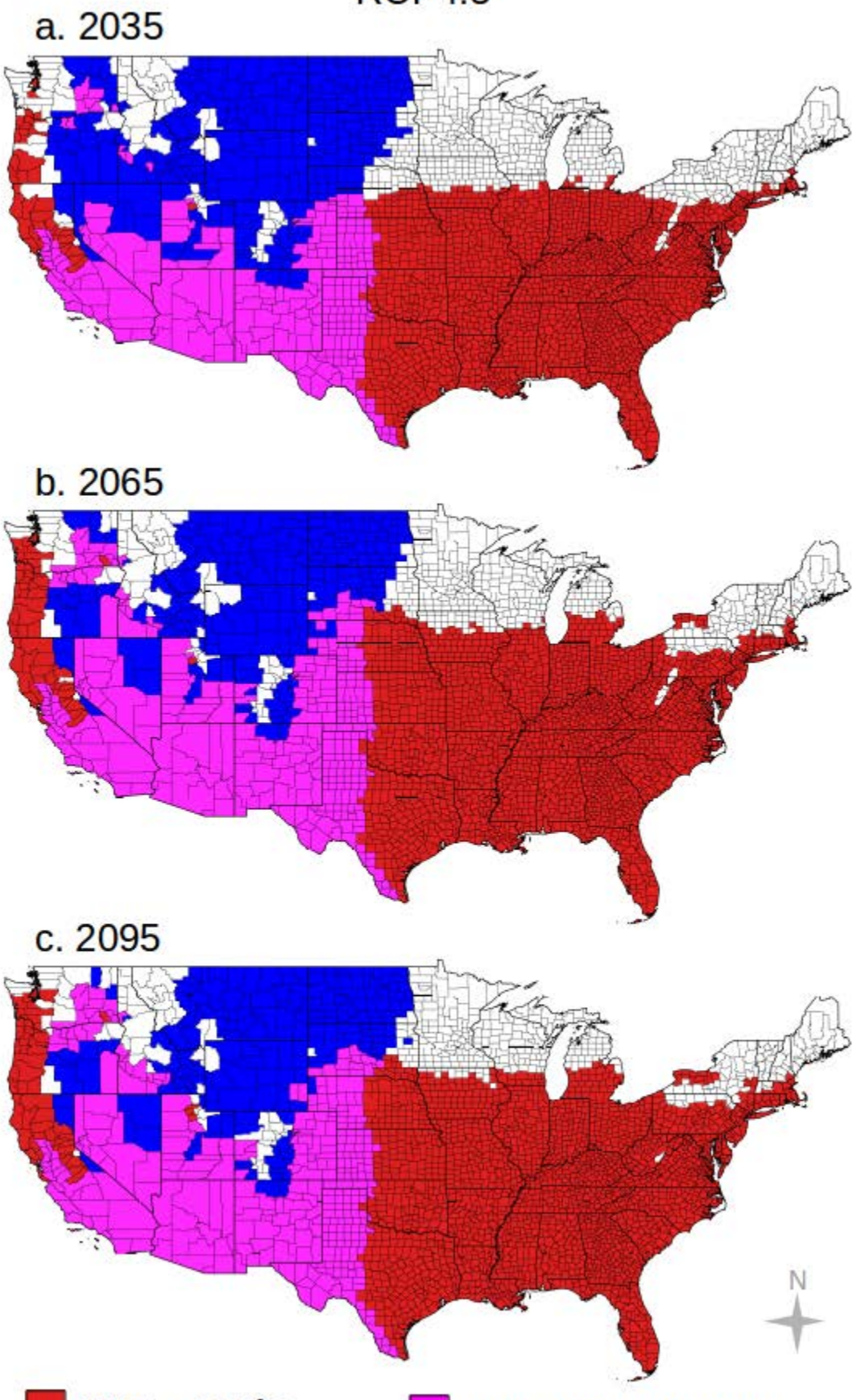
RCP4.5
a. 2035
b. 2065
c. 2095
N
MAT > 10.7˚C
Both thresholds met
MAP < 600 mm/year

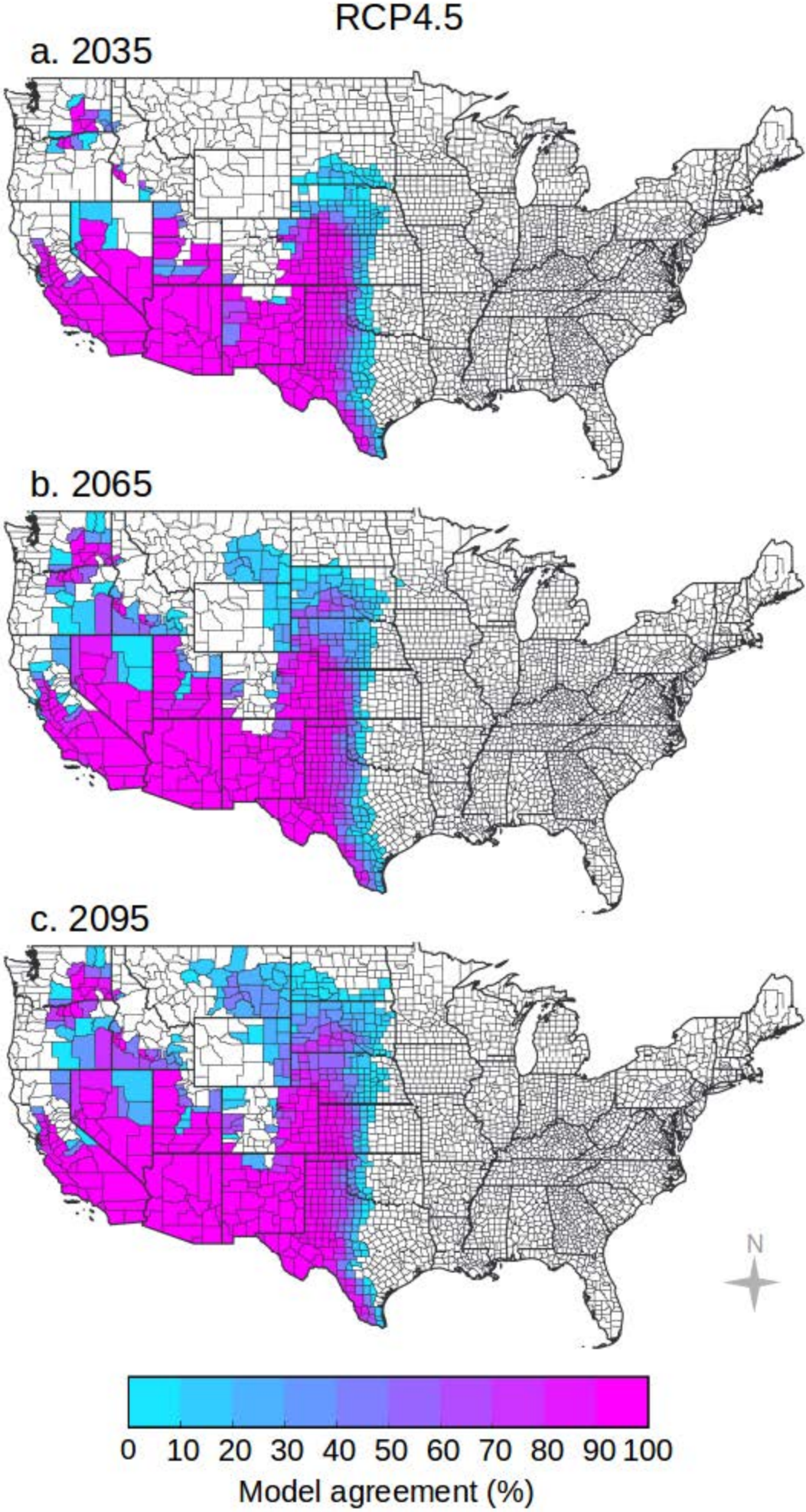
RCP4.5
a. 2035
b. 2065
c. 2095
N
0 10 20 30 40 50 60 70 80 90 100
Model agreement (%)

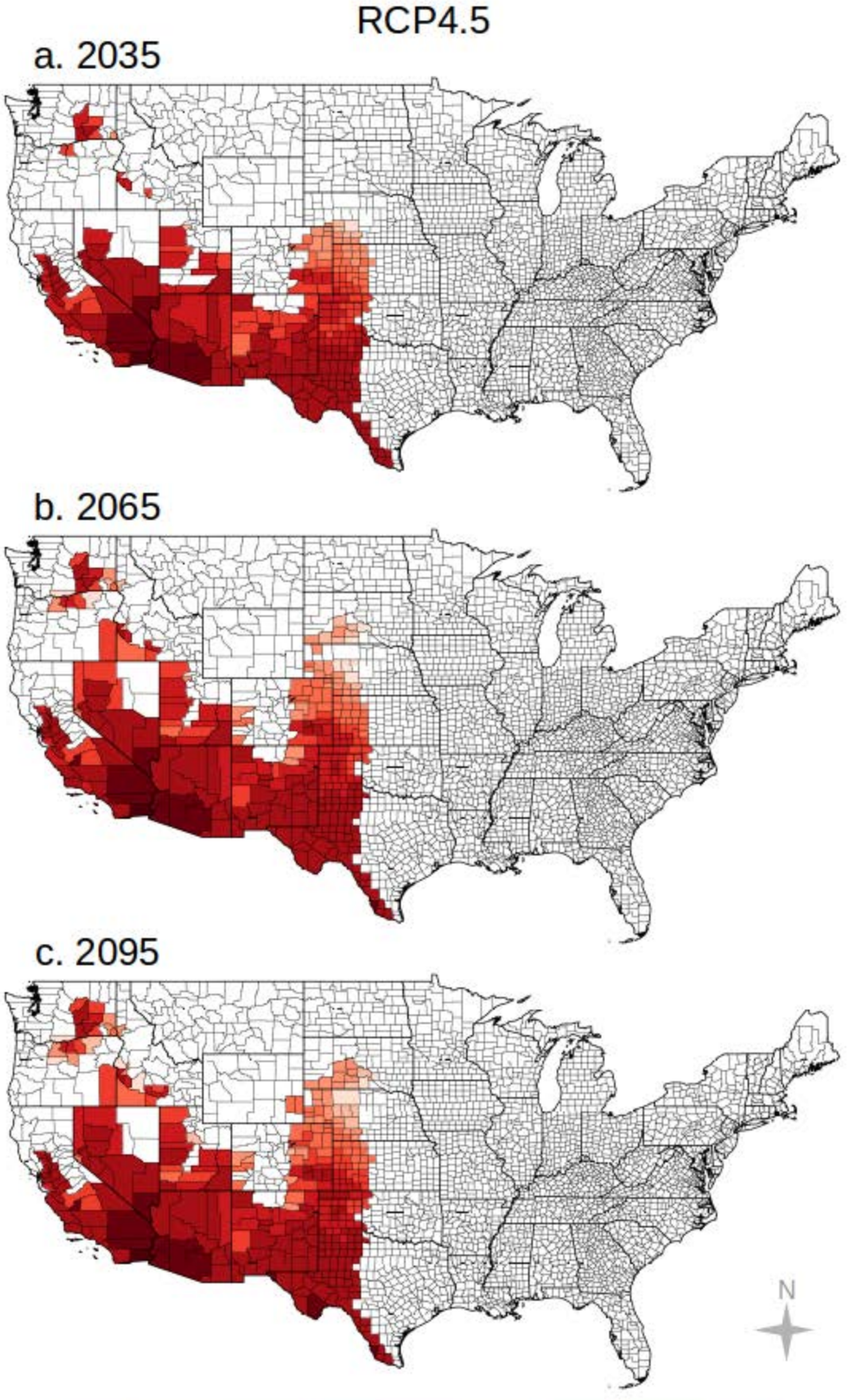
RCP4.5
a. 2035
b. 2065
c. 2095
N
0
5
10
20
30
40
50
100
150
200
90th Percentile potential Valley fever incidence
(cases per 100,000 population per year)